JAERI-M
8869

THE PRESENT STATUS OF ION SOURCE DEVELOPMENT AT JAERI

May 1980

Y. ARAKAWA, M. AKIBA*, M. ARAKI, H. HORIIKE, T. ITOH
M. KAWAI, M. KURIYAMA, S. MATSUDA, M. MATSUOKA,
Y. MIZUTANI,** T. OHGA, Y. OHARA, Y. OKUMURA,
J. SAKURABA,*** T. SHIBATA, H. SHIRAKATA and S. TANAKA

日本原子力研究所
Japan Atomic Energy Research Institute

この報告書は，日本原子力研究所がJAERI-Mレポートとして，不定期に刊行している研究報告書です．入手，複製などのお問合わせは，日本原子力研究所技術情報部（茨城県那珂郡東海村）あて，お申しこしください．

JAERI-M reports, issued irregularly, describe the results of research works carried out in JAERI. Inquiries about the availability of reports and their reproduction should be addressed to Division of Technical Information, Japan Atomic Energy Research Institute, Tokai-mura, Naka-gun, Ibaraki-ken, Japan.

JAERI-M 8869

The Present Status of Ion Source Development at JAERI

Yoshihiro ARAKAWA, Masato AKIBA*, Masanori ARAKI
Hiroshi HORIIKE, Takao ITOH, Mikito KAWAI
Masaaki KURIYAMA, Shinzaburo MATSUDA, Mamoru MATSUOKA
Yasuhiko MIZUTANI**, Tokumichi OHGA, Yoshihiro OHARA
Yoshikazu OKUMURA, Junji SAKURABA***, Takemasa SHIBATA
Hirofumi SHIRAKATA and Shigeru TANAKA

Division of Thermonuclear Fusion Research,
Tokai Research Establishment, JAERI

(Received April 28, 1980)

The ion source development for a JT-60 neutral beam injector is described. The experimental results obtained so far are also given.

Keywords; Outline, Ion Source, Development, JT-60 Neutral Beam Injector, Experimental Results

---

*) On leave from Kyushu University
**) On leave from Nissin Electric Co., Ltd.
***) On leave from Sumitomo Heavy Industries, Ltd.

JAERI-M 8869

原研におけるイオン源開発の現状

日本原子力研究所東海研究所核融合研究部

荒川　義博・秋場　真人*・荒木　政則・堀池　寛

伊藤　孝雄・河合視己人・栗山　正明・

松田慎三郎・松岡　守・水谷　泰彦**

大賀　徳道・小原　祥裕・奥村　義和・桜庭　順二***

柴田　猛順・白形　弘文・田中　茂

（１９８０年４月２８日受理）

ＪＴ－６０中性粒子入射装置用イオン源の開発状況について要約をおこなった。これまでに得られた実験結果を基にその概要を述べた。

＊）　特別研究生（九州大学）

＊＊）　外来研究員（日新電機）

＊＊＊）外来研究員（住友重機）

Contents

目　　次

1. Introduction

Neutral beam injection is one of the most powerful and effective methods for heating a tokamak plasma. To heat a JT-60 plasma up to 5 - 10 keV, a 20 MW neutral beam injection system which consists of fourteen injector units is planned and designed. Each of the two ion sources being used in these injector units is required to deliver a low divergent hydrogen ion beam of 35 A at beam energy of 75 keV for a duration of 10 sec.[1] The ion current density should be above 0.27 A/cm^2 over the large extraction grid of 12 cm × 27 cm with 40% transparency. The beam divergence angle within one degree is required to fit the acceptance angle of the JT-60 injection port. Furthermore, the ion source should be capable of producing high-power ion beams stably and repeatedly with such a long duration time. However, the ion sources of these specifications have not been developed yet. Our efforts must be concentrated on improvements of source plasma, beam optics and cooling of both extraction grids and plasma generator which appear to be the basic problems involved in the high power and long duration ion source.

The purpose of this paper is to present outlines and advanced processes of ion source development for the JT-60 injector. In section 2 the source plasma improvement based on experimental study is presented. Section 3 describes progress on beam optics of two-stage acceleration. Section 4 describes the experimental results and problems in the long pulse operation.

2. Improvement of Source Plasma

To produce well-collimated, high current ion beams, the plasma source should be capable of producing a dense, uniform, and quiescent plasma over the large extraction grid. Both noise level and spatial density variations should be below ±10% over the extraction area. Besides, the plasma source should have a high gas efficiency and an operational stability during a long pulse.

For this purpose, we have undertaken experiments to improve the source plasma by using a duoPIGatron, bucket and Lambdatron ion source.[2)3)] In this section results of the improvement of the source plasma are presented together with the developed ion source for the JFT-2 injectors.

2.1 DuoPIGatron Ion Source Development in the Early Stage

Historically, for the neutral beam research and development at JAERI, we built an ion source test stand called ITS-1 in Feb. 1975.[4)] Using this test stand, we developed and tested the duoPIGatron ion source for the old JFT-2 neutral beam injector in July 1976.[5)] This duoPIGatron ion source, which was almost the same as that developed at Oak Ridge National Laboratory,[6)7)] had the extraction grid diameter of 7 cm and produced a maximum drain current of 8A at 30 kV. The first modification of this prototype ion source is the geometrical scale up of the extraction grids to 10 cm diam, together with a larger arc chamber. With this source, we obtained a beam current of 9A at 27 kV. The second modification is the further geometrical scale up of the extraction grids to 15 cm diameter together with larger source plasma production electrodes. However, the maximum extraction current attained could not reach 10A although the extraction grid area was enlarged considerably. This unexpected result is attributed to the fact that there are spatial density variations and a considerable wall loss of charged particles in the source plasma production region. For this reason, we first tried to improve the uniformity of the source plasma.

Figure 1 is a sketch of the modified 15 cm diam. duoPIGatron ion source, which has a 14 mm diam. copper button located downstream of the intermediate electrode and a set of line cusp confinement magnets. We have already reported[2)] that the button of an optimum size can improve plasma uniformity without impairing the density level. Since it reduces the

passage of current carrying electrons, it intensifies the PIG discharge by increasing kinetic energy of ionizing electrons as they travel across the double sheath. The widened plasma production area by diverting the arc column from on-axis to off-axis also contributes to the uniform density distribution. On the other hand, line cusp confinement magnets play a role in raising the density level with a fixed arc input power[7]. This is because they confine energetic ionizing electrons and reduce the wall loss of charged particles. Figure 2 shows the density profiles of the source plasma with the 14 mm diam. button and line cusp confinement. The plasma density is measured by a Langmuir probe located 0.5 cm above the target cathode. As seen in this figure, the ion current density is up to 0.25 A/cm^2, uniform to $\pm$10% over the 15 cm grid diameter at an arc current of 305 A.

2.2 DuoPIGatron Ion Source for JFT-2 Neutral Beam Injector

Neutral beam injection into the JFT-2 tokamak has started at March in 1980. The total injection power is 1-2 MW which is several times larger than the ohmic heating power. The injector consists of two beam lines with four ion sources each of which can deliver a hydrogen ion beam of more than 20 A at 40 kV for 0.1 sec. To satisfy these specifications, we have developed an axisymmetric 18.5 cm diam. duoPIGatron ion source with a water-cooled buttom located in the neighborhood of the intermediate electrode and a set of line cusp confinement magnets around the arc chamber wall (See Fig. 3).

Each beamlet is focused to a point 2.5 m apart from the source by the aperture displacement technique. The source performance is shown in Table 1. The calorimetrically measured power fraction to the target which simulates the injection port of the JFT-2 tokamak is up to 80%. Consequently, we expect the total neutral beam power to the torus will be up to 1.7 MW with the neutralization efficiency of 0.6.

2.3 Coaxial DuoPIGatron Ion Source[8]

We have developed a new modified duoPIGatron ion source for the next step of the JFT-2 neutral beam injection, which is capable of delivering the injection power of more than 2 MW into the torus. Figure 4 shows a coaxial duoPIGatron ion source originally designed and developed at JAERI. The characteristic of this source is expressed as follows. A magnetic center pole located at the center of the nozzle (intermediate electrode)

actualizes hollow feeding of primary ionizing electrons to the arc chamber. Then it widens the plasma production area by diverting the arc column from on-axis to off-axis, thereby contributes to the uniform plasma distribution. The shapes and structures of both the magnetic center pole and the nozzle were optimized by numerical calculations of the magnetic field pattern. Typical density profiles of the source plasma are shown in Fig. 5. As seen in this figure, the ion saturation current density is up to 0.27 A/cm^2, uniform to ±10% over the 18.5 cm grid diameter at an arc current of 370 A. The source has been operated reliably producing a hydrogen ion beam of 30A at an accel voltage of 30 kV.

2.4 Rectangular DuoPIGatron Ion Source

As a developmental stage toward high energy long pulse ion source for JT-60 neutral beam injectors, we have made a rectangular duoPIGatron ion source with both a slot-shaped nozzle snout and a copper slot-shaped button (See Fig. 6). On the external chamber walls, a set of point cusp confinement magnets is equipped both to boost the plasma density and to improve the plasma uniformity, since the cusp field confines energetic ionizing electrons and reduces the wall loss of charged particles near the chamber walls. One end of the chamber is enclosed by a copper grid which simulates the plasma grid of a standard extraction system. Typical plasma density distributions are shown in Fig. 7. X and Y denote the distance from the center of the grid in the transverse and longitudinal directions, respectively.

The plasma density is increased by about 30% by the use of point cusp confinement, but the source plasma uniformity is not appreciably improved as expected. The reason is considered as follows. The nozzle snout of this source is too narrow to diffuse the ionizing electrons into the PIG region, thereby leads to the lack of plasma production near the chamber walls.

Oppositely, the use of a more widened nozzle snout leads to an excess of gas conductance of the nozzle and to a decrease of the gas pressure of the cathode region. Therefore it would be difficult to obtain a stable cathode plasma unless large amount of gas, which results in the unallowable pressure increase in the PIG chamber, is introduced into the cathode region.

2.5 Bucket Ion Source

It has been reported[9)10)] that bucket sources, recently developed elsewhere, produce quiescent, uniform, and dense plasmas. Since the bucket source has a large volume which is magnetic field free, with strong magnetic shielding of the surrounding walls, it offers better solutions particularly to the problems of plasma uniformity compared with duoPlGatron and reflex sources. Figure 8 shows a sketch of a rectangular bucket ion source which is of a 0.4 cm-thick, water-cooled chamber with 21 cm by 36 cm in length and 20 cm in depth. On the external chamber walls, a set of samarium-cobalt magnets are arranged in a continuous line-cusp configuration to generate a surface magnetic shield for primary electrons as well as for plasma ions. The source plasma is produced by primary ionizing electrons emitted from 16 pieces of 1.2 mm diam. tungsten filaments. As the plasma grid (target cathode) is isolated from the chamber by a ceramic spacer, the source can be operated conveniently either with the grid electrically floating or connected to the negative terminal of the filament. The rectangular extraction grids has 1032 apertures of 4.0 mm diameter over the 12 cm × 27 cm, which is almost the same as those being employed in the source for the JT-60 neutral beam injector. Using this source, we could easily obtain the uniform and dense plasma as shown in Fig. 9. Table 2 shows the typical performance characteristics for ion beam current of 24 A at 25 kV. After more than a thousand beam extractions, this source produced beam current of 30 A, which is a limiting value of the power supply of our test stand ITS-3.[11)]

2.6 Lambdatron Ion Source[12)]

A back plate of the arc chamber is exposed to a high heat flux density up to 1 kW/cm^2 due to the backstream electron beam.[25)] Furthermore, the surface heat flux of the back plate will be increased due to focusing of electron beam by the source magnetic field. This is the case for the source plasme generator such as duoPIGatron or bucket source where a spatially inhomogeneous magnetic field is applied for an efficient production of source plasma. In a quasi-DC source operation, it is necessary but quite difficult to remove such a high heat flux without any significant modification of the source structure. The major deficiency of the duoPIGatron source and the bucket source is that these sources may not be able to handle such a high heat flux. To overcome this problem, a new source

with a electron beam dump in the arc chamber is devised, which we named Lambdatron.[3)]

The back plate exposed to the backstream electron is modified with Λ-shaped beam dump to reduce the surface heat flux density. The ion loss area is approximately doubled compared with a conventional bucket source, and hence arc efficiency (ion beam current per arc power) will be reduced and the operating gas pressure in the arc chamber will be raised. The characteristics of this new source were compared experimentally with those of the conventional bucket source, using a circular ion source shown in Fig. 10. The line cusp field arrangement is composed of 18 columns of Co-Sm magnets of 20 cm long. The measurement of the maximum magnetic field on the wall surface shows B = 1.2 kG. We used 9 pieces of hairpin tungsten filaments for hot cathodes. The plasma grid has 1052 apertures of 4.0 mm diameter over the central 18.5 cm diameter area. The plasma density obtained is uniform within ±5% over the grid area. Table 3 shows typical performance characteristics of both the sources for ion beam current of 30A at 30kV. Here, the gas pressures in the arc chamber are fixed to 3.5 mtorr for the conventional bucket source and 6.0 mtorr for Lambdatron, where the arc efficiency takes maximum. We had to permit the 40% decrease of the arc efficiency when we used the Lambdatron instead of the conventional bucket source, while no significant change in atomic fraction was observed. Consequently, it is envisaged that this source is a candidate for the source plasma generator of the JT-60 ion source.

3. Beam Optics of Two-Stage Acceleration System

A large-sized tokamak such as JT-60 demands a high beam power at high energy (75 keV). If the ion source has a configuration of single stage acceleration, the decrease of beam power flux density is inevitable with such a high acceleration energy because of the electrical breakdown problem between extraction grids. This problem can be solved by employing a multiple acceleration system.

Furthermore, beam divergence should be low enough (less than one degree) to keep high injection efficiency against geometrical losses due to the long beam line and the limited injection port between the toroidal coils.

To develop ion sources of these specifications, we have constructed a 100 kV test stand called ITS-2.[13] The two-stage series power supplies are capable of delivering ion beams up to 40 A at 100 kV level. By making use of this test stand, our effort have been concentrated on beam optics, and cooling of the extraction grids which appear to be the basic problems involved in high power and long duration ion source development. In this section, the beam optics of the two stage acceleration system is presented.

3.1 Beam Optics by Computer Simulation[14]

A computer simulation code for cylindrically symmetric ion beams has been developed for the design of the ion-extraction system and the optimum operating condition of an ion source. In the simulation model, the beam emitter surface is determined self-consistently in such a way that the ion saturation density is equal to that of the space-charge-limited current density. The potential of the emitter corresponds to that of the first electrode in contact with the source plasma. Finite ion and electron temperatures of the source plasma are taken into consideration as the initial conditions of the beam trajectories. The ion starts from the emitter with an initial energy corresponding to 3.5 times the electron temperature. The ion temperature determines the initial direction of the emitting ion, which is obtained by the assumption of the drift-Maxwellian ion distribution at the emitter. The accelerated ions that pass through the zero equipotential surface under the grounded electrode do not suffer from space-charge expansion because of the presence of an electron cloud produced by the collisions of beam ions with the residual cold neutral gas. Therefore, the beam divergence is defined on this surface.

To investigate the validity of this code, computed beam divergence

(rms angle) are compared with the experimental data (1/e half-widths) for the same configuration of the extraction electrodes.
To match the computational results with the experimental data, it is important to assume that no ions are emitted from the peripheral region of the emitter, whose width corresponds approximately to the thickness of the wall sheath which is about 10 times the Debye length of the source plasma. This may be due to the fact that ions in the wall sheath are mainly accelerated to the wall by the potential drop between the source plasma and the wall and impinge on the wall before they are accelerated toward the downstream region.

Figure 11(a) shows the dependence of the beamlet minimum divergence ω_{min} on the field intensity ratio f (the ratio of the electric fields in the first and second gap), for the fixed acceleration voltage of 75 kV, where the breakdown limit for the gap distance is neglected. Although it does not cover enough ranges of the parameters, one finds that ω_{min} decreases almost proportionally with decreasing f and does not depend strongly on the aspect ratio and on the gap ratio for the fixed values of f.

3.2 Experimental Study of Beam Optics

According to the results of analytical estimation in the thin lens approximation or two-dimentional computer simulation of an ion beam trajectories, the field intensity ratio f is an important parameter for the beam optics in the two-stage acceleration system. Here, we try to study the effect of f on the beam optics experimentally.[15)]

The experiments are performed with a duoPIGatron source with two-stage acceleration system, which is shown in Fig. 12. The two-stage acceleration system is composed of four grids called plasma grid, gradient grid, suppressor grid and exit grid, respectively (See Fig. 13). The plasma grid in contact with a source plasma is held at a positive high potential corresponding to the desired beam energy V_{tot} ($=V_{ext}+V_{acc}$). The potential V_{acc} is applied at the gradient grid. The suppressor grid is biased at negative voltage V_{dec} to suppress the electron backstreaming from the downstream beam plasma region. In the present experiments, V_{dec} is fixed to 1.6 kV. The exit grid is ground electrically. The electric currents into the plasma, the gradient and the suppressor grid are denoted as I_p, I_g and I_{dec}, respectively. The polarity of the current I_g is also shown in Fig. 13. The accel drain current is expressed as I_{acc}, and is equal to

$I_p - I_g$. The extraction grids are made of 15 cm diam. copper disk with 83 apertures over central 5 cm diam. area. The aperture diameter is 3.5 mm in the plasma and the gradient grid, while it is 4.0 mm in the suppressor and the exit grid. The transparency of the grids is 43 %. The grid thickness is 2.0 mm in the plasma and the exit grid and 1.5 mm in the gradient and the suppressor grid. The extraction and the acceleration gap distance denoted by d_{ext} and d_{acc}, respectively, are changed in the range of 4.5 - 8.0 mm. The decel gap distances is fixed to 2.5 mm.

The beam divergences are measured as functions of gap distances d_{ext} and d_{acc} and total beam energy $V_{ext}+V_{acc}$ in the range of drain current I_{acc} = 0.1 - 1.6 A. Figure 14 shows the beam divergence as a function of perveance per hole in the case of $d_{ext} = d_{acc} = 6$ mm, and $V_{ext} + V_{acc} = 50$ keV, where perveance per hole is defined by $I_{acc}(V_{ext} + V_{acc})^{-3/2}$ divided by the number of apertures. This result shows that the reduction of the ratio V_{ext}/V_{acc} makes the minimum beam divergence ω_{min} decrease for the fixed gap distances, while we must allow the reduction of optimum perveance P_{opt}. The latter is defined by the perveance that gives the minimum beam divergence when the extraction current I_{acc} is changed. It also shows that the divergence increases very gradually above the optimum perveance. Such tendency is not observed in the single-stage acceleration. This is preferable to obtain a low divergent and high perveance beam. Figure 15 summarizes wide variety of data from the view point of the dependence of minimum beam divergence and optimum perveance on the field intensity ratio. From this figure, it is seen that the decrease of f makes ω_{min} and P_{opt} decrease, as is expected by the analytical and numerical estimation.

3.3 Aperture Shaping Effect on Beam Optics

Effects of aperture shape on beam optics have previously been studied in some detail using ion sources with a single-stage, accel-decel structure.[16)17)18)] Some aperture shape in the plasma electrode makes a beam with very low divergence (smaller than one degree). In the two-stage configuration, the aperture shape in the gradient grid also has great influence on beam optics. When the field intensity ratio is smaller than unity, the gradient grid acts as a positive lens. In such a case, the aberrations of the lens can be reduced by chamfering the aperture edge on the downstream side. Figure 16 shows the types of aperture shape studied. All the above experiments are made by using the type 1 grid.

Figure 17 shows the beam divergence as a function of perveance per hole for aperture types 1 - 4, where $d_{ext} = d_{acc} = 6$ mm, $V_{ext} = 15$ kV and $V_{acc} = 35$ kV. Chamfering of apertures in the gradient grid together with that in the plasma grid is indeed effective, and the beam divergence is reduced by about 0.5 degree in the type 4 grid, compared with the type 1 grid.

3.4 Beam Focusing by Aperture Displacement[12) 24)]

In the JT-60 neutral beam injector, the increase of the injection power by about 13 % of the total beam power will be expected by the focusing of indivisual beamlets to the injection port. As one of the most promising methods, we have investigated experimentally the focusing by aperture displacement. In the two-stage accelerator, there are three cases of aperture displacement; i.e. the displacements of aperture in the plasma grid, in the gradient grid, and in the suppressor grid. In the experiment where 4.0 mm diameter aperture is used, the deflection angle increases almost linearly with the displacement of aperture. This is somewhat different from that obtained at ORNL[19)]. Figure 18 shows the dependence of each deflection characteristic on the field intensity ratio which determines two-stage beam optics. Here, the triangular, rectangular, and circular points indicate the displacements of apertures in the plasma grid, in the gradient grid, and in the suppressor grid, respectively. The lines indicate the results obtained analytically by thin lens approximation for each case. From this figure, we can see that the displacement of aperture in the suppressor grid is more than adequate. This is due to the fact that the deflection characteristic scarcely depends on the field intensity ratio, that is to say, the focal point does not change over a wide range of ion source operation conditions.

3.5 Beam Extraction from Multiple-Slots[20)]

One way of producing higher current ion beams is to raise a geometrical transparency of extraction grids. In the case of grids with a number of small circular apertures, it is difficult to have grids with more than 40% transparency, since grids should have a series of water cooling pipes on its surface for long pulse operation. On the other hand, in the case of grids with multi-slots, higher transparency ($\sim$60%) can be obtained easily, which enables us to extract higher currents from a limited grid area. To make assessments of this system, we have designed and tested the multi-slots

extracter which has the transparency of 64%.

The front view of the plasma grid is shown in Fig. 19. The grid contains 8 slots, which is 4 mm wide and 5 cm long with ronded ends, forming a square 5cm × 5cm array. Only the plasma grid is made of copper rods on which copper cooling pipes of 1.5 mm outer diam. are brazed, while other grids are made of pipes 2.0 mm outer diam. The downstream side of the plasma grid is shaped so as to produce low divergent beams by reducing the aberrations. Fig. 20 shows the divergences as a function of perveance per hole, where preveance per hole is defined by $I_{acc}(V_{ext}+V_{acc})^{-3/2}$ divided by the number of apertures. The divergence in the direction parallel to the slots ranges from 0.7° to 0.9°. This value is so small that the 5-cm length of the slots contributes significantly to the beam size at the distance 2.0 m from the extractor.

As reported in reference 14, the field intensity ratio "f" defined by $V_{ext}d_{acc}/(V_{acc}+V_{dec})\,d_{ext}$ is an important parameter for the two-stage beam optics. The minimum beam divergence is improved with the decrease of "f", while one must allow the decrease of the optimum perveance, the perveance at which the divergence is minimum. Such tendency is also observed in the case of slots as shown in Fig. 21, where $V_{tot}=V_{ext}+V_{acc}$= 30, 50 and 60 kV, f = 0.31 and 0.47.

Comparing these results with the results for the circular apertures, it is evident that the beam quality in the direction perpendicular to the slots is considerably worse. This is considerd as follows; in the case of circular apertures, the beam receives two-dimentional focusing, while one-dimentional in the case of slots. The space charge effect of beamlet-beamlet interaction may deflect the outermost beamlets in the case of slots.

4. Long Pulse Beam Extraction

In attaining long pulse beams at high energy, it is important to slove the problems concerning accelerator loading and loading due to backstream electrons striking the back plate of the plasma generator, and concerning cathode durability. To investigate the problems and to establish the technology for long pulse beam extraction, we fabricated and tested a quasi-DC ion source which can produce 70 keV, 5A hydrogen ion beam for 10 sec. In this section, we will describe the experimental results and the problems limiting the beam pulse length. Measurements of the time dependences of atomic fraction and impurity level during the long pulse operation are also described. In the last of this section, we will describe the experimental results of a hollow cathode.

4.1 Heat Loading of Extraction Grids in Two-Stage Accelerator[12) 26)]

One of the critical problems which limit the beam pulse length is the heat loading and the removal of the heat on the extraction grids. To investigate this problem, we have designed and fabricated an axisymmetric 75 keV, 6A, 10 sec ion source, a modified duoPIGatron with a two-stage accelerator (See Fig. 22).

The ion accelerater consists of a cylindrical hard sealed alumina ceramic insulator (ID = 316 mm, OD = 353 mm) and two-stage extraction grid assembly. Each grid made of oxygen free copper has 191 apertures over the central 10 cm diameter area with each aperture of 4.0 mm in diameter and then the transparency is 31 % (see Fig. 23(a)). On the surface of each grid, copper pipes of 1.8 mm in outer diameter and 1.2 mm in inner diameter are brazed alternately with rows of apertures. Each grid is supplied with pressurized pure water (10 atm.) at a flow rate of 10 liter/minute. The cross sections of each aperture are shown in Fig. 23(b).

Figure 24 shows the heat loading on each grid measured calorimetrically as a function of ion beam drain current I_{acc}, where final beam energy V_{tot} is 75 keV, and the gas pressure at the entrance of the neutralizer cell P_N is 1×10^{-3} Torr. The loadings are normalized by the total beam power defined by $I_{acc} \times V_{tot}$. The loadings become minimum at a beam current I_{acc} = 5-6 A, where the beam divergence is minimum. These heat loadings increase almost linearly with P_N. At I_{acc} = 5-6 A and $P_N = 3.6 \times 10^{-3}$ Torr which gives 90 % neutralization for 75 keV proton beam, the heat loadings on the plasma

grid, the gradient grid, the suppressor grid and the exit grid are 1.5%, 1.1 %, 0.3 % and 1.0 % of the total beam power, respectively. The loading of 1.5 % corresponds to the heat flux density of 125 W/cm^2 at grid plate surface and 143 W/cm^2 at cooling surface of pipes. This heat flux is sufficiently below our design value for quasi-DC source operation as indicated in Ref. 21.

The heat loading on the grid may cause distortion of the grids, which affects the beam optics. To investigate this effect, the beam profile was measured by multi-channel photo beam monitor[22] during 10 sec. The monitor has 17 slots and the light of the beam is detected by photo diodes installed in each slot. The measurement indicates that no significant change in beam profile was observed during 10 sec.

4.2 Heat Loading of the Back Plate of the Plasma Generator[12) 26)]

One of the critical problems for quasi-DC beam extraction is the electron backstream into the source plasma region. We measured the total heat loading on the back plate of the plasma generator, where the heat loading due to arc power and radiation from filaments are subtracted. Figure 25 shows the results, where V_{tot} and I_{acc} are fixed to 75 kV and 5 A, respectively. The loading increases linearly with the pressure and the dependences agree well with the calculated one. To avoid damage to the back plate and the filaments in quasi-DC operation, we had to keep the heat flux below 2.5 % of the total beam power by limiting the pressure in the accel gap below several mTorr.

4.3 Mass Analysis of Long Pulse Beam[12)]

The time dependences of atomic fraction and impurity level including the effect of source conditioning are investigated on the ion beam extracted from the 10-sec source. The line density of the cold hydrogen gas between the ion source and the mass analyzer is fixed to 0.39 Torr·cm, which gives 90 % neutralization for 75 keV proton beam.

Table 4 shows the typical beam fraction and impurity levels at 75 kV, 6.2 A, where mass analysis are performed at 0.5 sec after the beam is turned on and the pressure in the arc chamber is ∿10 mTorr. The atomic fraction of the primary ion beam is calculated by the cross section data; i.e. H_1^+: H_2^+: H_3^+ = 66:22:12. On the other hand, it is difficult to estimate the flux of each neutral impurity, because of the insufficient cross section

data.

No change in atomic fraction during 10 sec was observed. However, impurity level changes appreciably during the pulse. Figure 26 shows the time dependence of impurity spectra. Impurity ions related to oxygen (M = 13.5-19) decreases with time, while impurities related to carbon (M = 8.5-16) increases during the pulse. The time dependence of H_2O^+ (M = 18) level is shown in Fig. 27(a). In Fig. 27(b), the accel voltage is cut off for the initial 1.3 sec, while arc discharge is performed during the cut off time. This result indicates that the impurity decreases appreciably during the initial 1 sec, and the arc flushing just before the beam extraction is very effective to decrease the impurity level related to oxygen (M = 13.5-19). With the W-filaments instead of the oxide coated tantalum filaments, any significant change in these impurity level was not observed. These impurities seems to come from the wall of arc chamber made of oxygen free copper.

In the JT-60 tokamak, the neutral beam will be injected every 10 minutes. The long time interval between the shots will be sure to increase the impurities. The measurement indicates that the impurities related to oxygen and carbon are doubled during the beam off time of only about 100 sec. However, the conditioning of the source can reduce the impurities. Figure 28 shows the effect of various conditioning modes on the impurity level. It is noticeable that the arc discharge just before the ion extraction like Mode VI,VII can reduce the impurity level appreciably.

4.4 Hollow Cathode

The JT-60 tokamak device requires neutral beam heating for up to 10 seconds duration. Long pulse operation of ion sources with high current arc requires a high degree of reliability and durability to cathodes. Furthermore cathodes are required to have a low heater power, long lifetimes, and a small surface exposure to the source plasma for minimum ion losses. Conventional cathodes seldom satisfy all of these criteria. For example, tungsten hairpin filaments require large amounts of heater power, are fragile after heating, and have high thermal stresses as they operate at high temperatures approaching 3000°K. In addition, they may be damaged by either ion bombardment or arc spotting as they are directly exposed to the dense source plasmas.

A hollow cathode, such as designed and developed at UCLA[23], seems to be the most adequate one for such a long-pulse ion source. The reason is as follows. An electron emitter of this cathode is indirectly heated and

requires low input power. It is positioned inside a cathode assembly, which leads to the protection of the emitter suffering from both ion sputtering and arc spotting. In addition, a hollow cathode is capable of maintaining a high arc current, since the cathode plasma itself acts as an electron source in place of the electron emitter.

We have fabricated and tested a bucket source with a hollow cathode as shown in Fig. 29. Preliminary experiments were undertaken applying it to the 18.5 cm grid diam. bucket source described in the previous section. Details of the cathode assembly are shown in Fig. 30. As an electron emitter, a cylindrical impregnated tungsten was used, which is heated from the inside by a noninductively wound tungstan coil. In operation of this cathode, we have found that a considerable gas flow rate (more than 20 Torr·ℓ/s)are required to start a hollow cathode discharge, which leads to unfavorable effects such as decreases of gas efficiency, arc efficiency and significant increases of heat loadings of both the extraction grids and the plasma generator. However, we found that a gas flow rate can be reduced below 5 Torr·ℓ/s if once arc discharge is turned on. Therefore, we have modified the gas feed line so that mass flow rate has the time dependence as seen in Fig. 31. Using this hollow cathode with a 10 mm diam. orifice, we obtained a stable arc operation repeatedly. Hollow discharges were maintained during 1 sec with arc current up to 380 A. Consequently, it can be expected that this hollow cathode will be used as the cathode of the JT-60 ion source.

5. Summary

This paper has summarized the outline of the ion source development for the JT-60 neutral beam injector. The process and advances in ion sources are shown chronologically in Table 5. At first we constructed and tested the 7 cm diam. duoPIGatron ion source installed in the JFT-2 tokamak device in 1967, which was the beginning of the neutral beam injection experiment at JAERI. On the next step our efforts have been concentrated on the three main subjects, namely, source plasma production, beam optics and a long pulse operation; these subjects should be overcome to develop the ion source for the JT-60 injector. At present the improved source plasma has almost attained the required level, as confirmed by the beam extraction experiments.

We have also investigated beam optics of the two-stage acceleration system. We can develop the two-stage ion source which produce high energetic ion beams with low beam divergence (one degree). In addition, heat loading of the extraction grids, which is one of the critical problems involved in the long pulse operation, has been investigated experimentally. The loading of the grids could be reduced below our design value with the help of improvement of beam optics. However there exist some uncertain problems in a long pulsed operation, that is, the distortion of extraction grids by thermal expansion and thermal damage of cathodes by the high-current arc discharge, etc. The solution to these problems will lead to the production of reliable and endurable ion source for the JT-60 injector.

Acknowledgement

The authors are grateful to Drs. S. Mori and Y. Obata for their support and encouragement.

5. Summary

This paper has summarized the outline of the ion source development for the JT-60 neutral beam injector. The process and advances in ion sources are shown chronologically in Table 5. At first we constructed and tested the 7 cm diam. duoPIGatron ion source installed in the JFT-2 tokamak device in 1967, which was the beginning of the neutral beam injection experiment at JAERI. On the next step our efforts have been concentrated on the three main subjects, namely, source plasma production, beam optics and a long pulse operation; these subjects should be overcome to develop the ion source for the JT-60 injector. At present the improved source plasma has almost attained the required level, as confirmed by the beam extraction experiments.

We have also investigated beam optics of the two-stage acceleration system. We can develop the two-stage ion source which produce high energetic ion beams with low beam divergence (one degree). In addition, heat loading of the extraction grids, which is one of the critical problems involved in the long pulse operation, has been investigated experimentally. The loading of the grids could be reduced below our design value with the help of improvement of beam optics. However there exist some uncertain problems in a long pulsed operation, that is, the distortion of extraction grids by thermal expansion and thermal damage of cathodes by the high-current arc discharge, etc. The solution to these problems will lead to the production of reliable and endurable ion source for the JT-60 injector.

Acknowledgement

The authors are grateful to Drs. S. Mori and Y. Obata for their support and encouragement.

References

1) S. Matsuda et al. ; JAERI-M 7655 (1978)
2) Y. Arakawa et al. ; JAERI-M 8088 (1979)
3) J. Sakuraba et al. ; JAERI-M 8740 (1980)
4) S. Matsuda et al. ; JAERI-M 6431 (1976)
5) T. Sugawara et al. ; JAERI-M 7043 (1977)
6) W.L. Stirling et al. ; ORNL/TM-5662 (1976)
7) R.C. Davis et al. ; ORNL/TM-4657 (1974)
8) H. Horiike et al. ; To be published
9) A.P.H. Goede and T.S. Green ; Proc. 8th Symp. Eng. Prob. of Fusion Research (1979)
10) L.A. Biagi. et al. ; Proc. 8th Symp. Eng. Prob. of Fusion Research (1979)
11) T. Itoh et al. ; JAERI-M 8537 (1979)
12) Y. Ohara et al. ; Proc. 8th Symp. Eng. Prob. of Fusion Research (1979)
13) T. Ohga et al. ; JAERI-M 7604 (1978)
14) Y. Ohara ; J. Appl. Phys. Vol. 49 No.9 (1978)
15) Y. Ohara et al. ; Proc. 7th Symp. Eng. Prob. of Fusion Research (1977)
16) W.S. Cooper, K.H. Berkner and R.V. Pyle ; Nucl. Fusion 12 (1972) 263
17) E. Thompson ; Proc. 2nd Symp. on Ion Sources and Formation of Ion Beams 1974 Paper II-3.
18) L.R. Grisham et al. ; Rev. sci. Instrum. 48 (1977) 1037.
19) W.L. Gardner et al. ; Rev. Sci. Instrum. 49 (1978) 1214.
20) Y. Okumura, H. Horiike and Y. Ohara ; 3rd Symp. on Ion Source and Application Technology (1979)
21) H. Horiike et al. ; To be published
22) M. Kawai et al. ; JAERI-M 8778 (1980)
23) D.M. Goebel, J.T. Crow and A.T. Forrester ; Rev. Sci. Instrum. Vol. 49 No.4 (1978)
24) Y. Okumura et al. ; Rev. Sci. Instrum. 51 (1980) 471
25) Y. Ohara et al. ; to be published in J. Appl. Phys. 51 (1980)
26) Y. Okumura et al. ; to be published in Rev. Sci. Instrum. 51 (1980)

TABLE 1 PERFORMANCE CHARACTERISTICS OF A MODIFIED DUOPIGATRON ION SOURCE WITH 185 mm DIAMETER ACCELERATOR

FILAMENT CURRENT	60 A x 12
ARC VOLTAGE	80 V
ARC CURRENT	250 A
ACCEL VOLTAGE	30 kV
ACCEL CURRENT	25 A
DECEL VOLTAGE	-1.6 kV
DECEL CURRENT	2.8 A
DURATION TIME	0.1 sec
POWER FRACTION TO TARGET	80 %
$H^+ : H_2^+ : H_3^+$	59:28:13
IMPURITY (C,O)	1 %
ARC EFFICIENCY	1.25

TABLE 2 PERFORMANCE CHARACTERISTICS OF A RECTANGULAR ION SOURCE

FILAMENT CURRENT	1400 A
ARC VOLTAGE	85 V
ARC CURRENT	640 A
ACCEL VOLTAGE	30 kV
ACCEL CURRENT	24 A
DECEL VOLTAGE	-1.6 kV
DECEL CURRENT	1.3 A
DURATION TIME	0.1 sec
$H^+ : H_2^+ : H_3^+$	75:28:7
ARC EFFICIENCY	0.44

TABLE 3 TYPICAL PERFORMANCE CHARACTERISTICS OF THE BUCKET SOURCE AND LAMBDATRON FOR ION BEAM CURRENT OF 30 A AT 30 kV.

	BUCKET	LAMBDATRON
FILAMENT CURRENT	720 A	1080 A
ARC CURRENT	260 A	460 A
ARC VOLTAGE	100 V	95 V
PRESSURE	3.5 mTorr	6 mTorr
$H^+ : H_2^+ : H_3^+$	70 : 20 : 10	70 : 20 : 10
ARC EFFICIENCY	1.1 A/kW	0.7 A/kW

TABLE 4 SPECIES OF 75kV, 6.2A ION BEAM.

M	%	
1/3	10.7	$H^+(1/3\,E)$
1/2	17.9	$H^+(1/2\,E)$
1	60.3	$H^+(E)$
4/3	0.6	$H_2^+(2/3\,E)$
2	1.2	$H_2^+(E)$
3	0.24	$H_3^+(E)$
0~3	90.94	
8.5	0.015	$CH_n^+ \rightarrow C^+, CH_m^+$
9	0.039	
10.0	0.024	
10.8	0.024	
11.2	0.030	
12	0.011	C^+
13	0.015	CH^+
13.5	0.24	$H_3O \rightarrow O^+$
14,14.2	0.55	$CH_2^+, H_2O^+ \rightarrow O^+$
15	0.17	$CH_3^+, OH^+ \rightarrow O^+$
16	0.095	O^+
17	0.015	OH^+
18	0.015	H_2O^+
19	0.010	H_3O^+
8~19	1.35	
23	0.001	Na^+
24	0.002	Mg^+
27	0.0001	
28	0.0003	N_2^+
32	0.001	O_2^+
34	0.0003	
35	0.0003	
39	0.0005	
40	0.0006	Ca^+
44	0.0003	
23~44	0.006	

M	%	
63	0.008	$^{63}Cu^+$
64	0.003	$^{64}Zr^+$
65	0.004	$^{65}Cu^+$
66	0.0015	$^{66}Zn^+$
68	0.001	$^{68}Zn^+$
107	0.0006	$^{107}Ag^+$
109	0.0005	$^{109}Ag^+$
160	0.0007	
63~160	0.019	
-1/3	3.28	$H^-(1/3\,E)$
-1/2	2.09	$H^-(1/2\,E)$
-1	0.48	$H^-(E)$
0~-1	5.85	
-8.5	0.01	$CH_n^+ \rightarrow C, CH_m^-$
-9	0.01	
-10.0	0.005	
-10.8	0.005	
-11.2	0.005	
-12	0.030	C^-
-13.5	0.43	$H_3O^+ \rightarrow O^-$
-14.2	0.85	$H_2O^+ \rightarrow O^-$
-15	024	$OH^+ \rightarrow O^-$
-16	0.09	O^-
-8~-16	1.67	
-24	0.0005	
-32	0.0002	O_2^-
-24~32	0.0007	

TABLE 5 TYPES OF EXTRACTION GRID DEVELOPED AND BEING DEVELOPED AT JAERI

Ion Source Development at JAERI

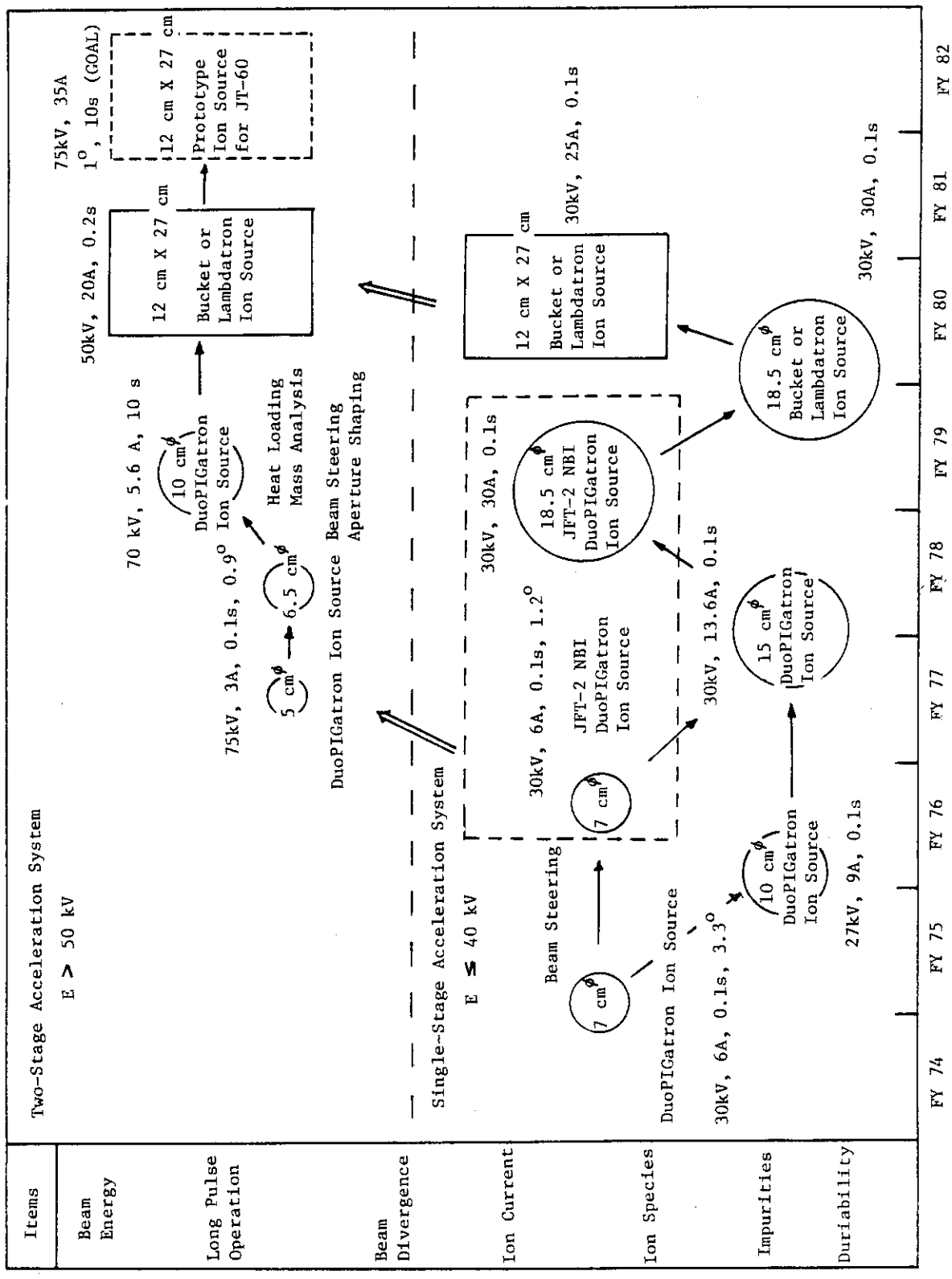

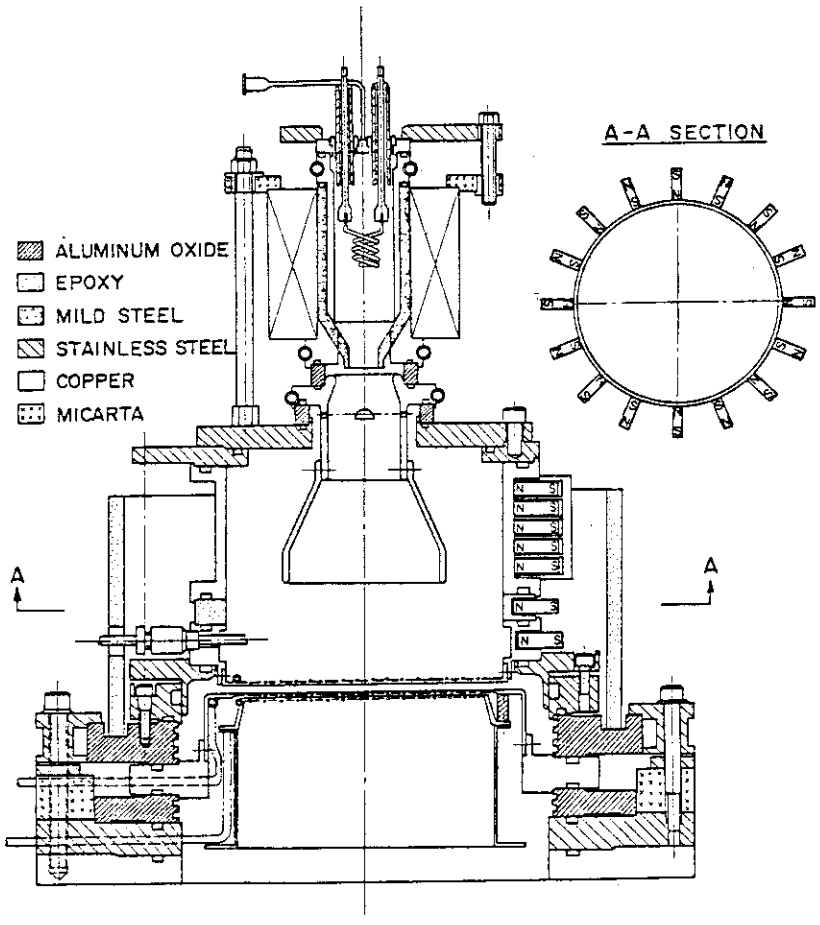

Fig. 1 DuoPIGatron ion source with 15 cm diam. grid.

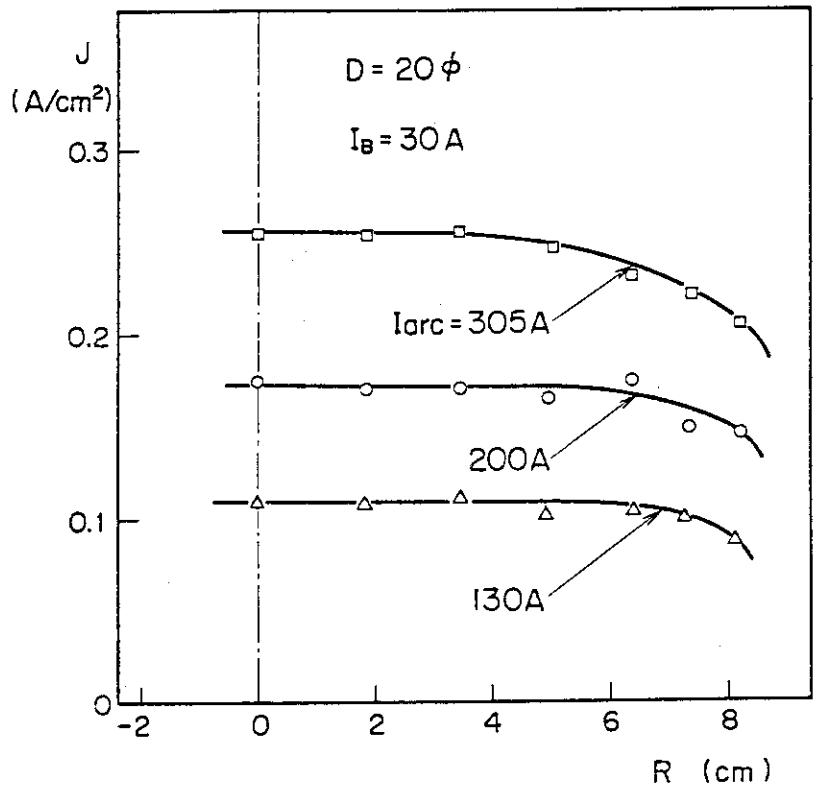

Fig. 2 Improved density profiles of the source plasma in the 15 cm diam. source.

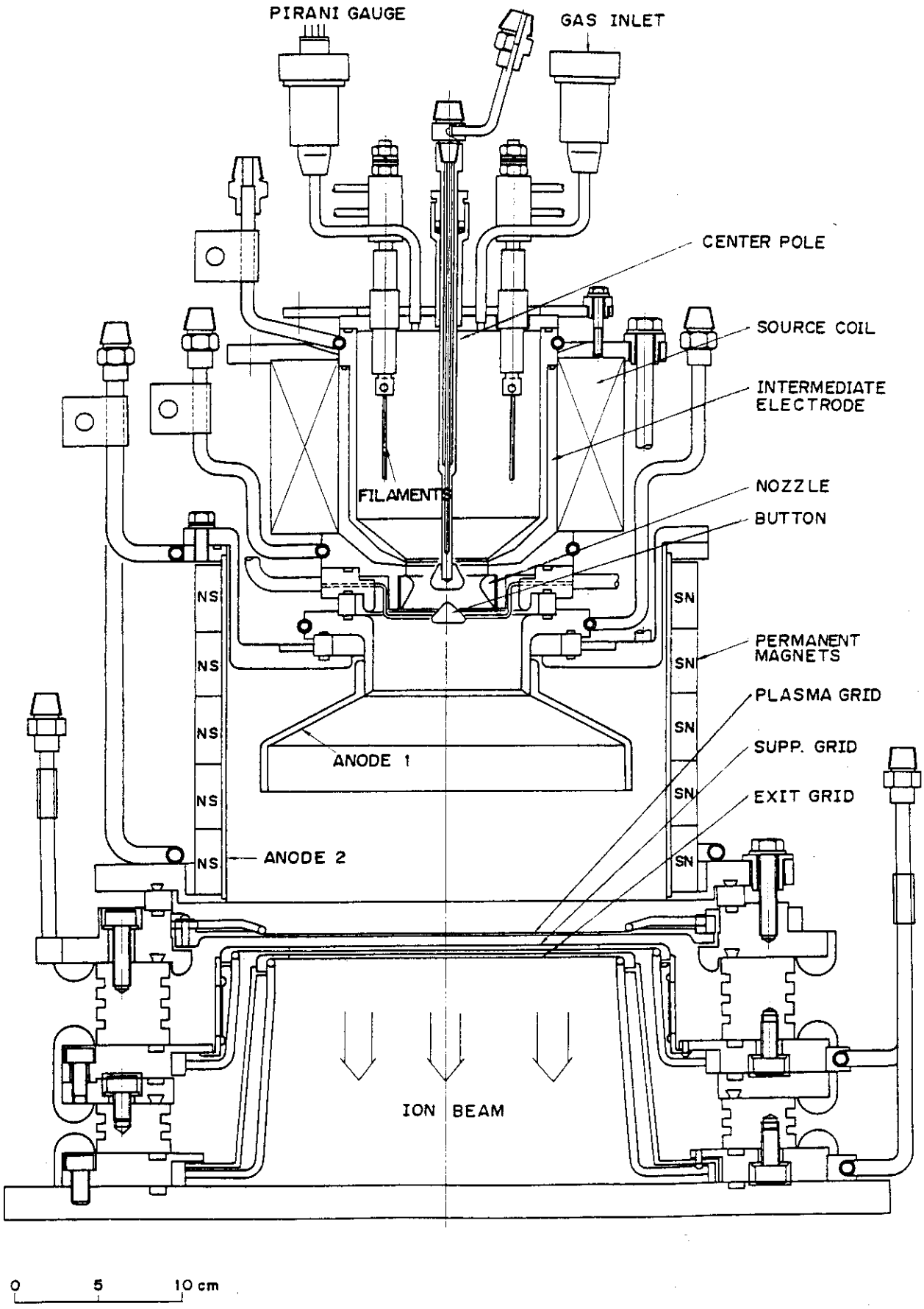

Fig. 3 DuoPIGatron ion source for JFT-2 neutral beam injector (both axial button and center pole are shown).

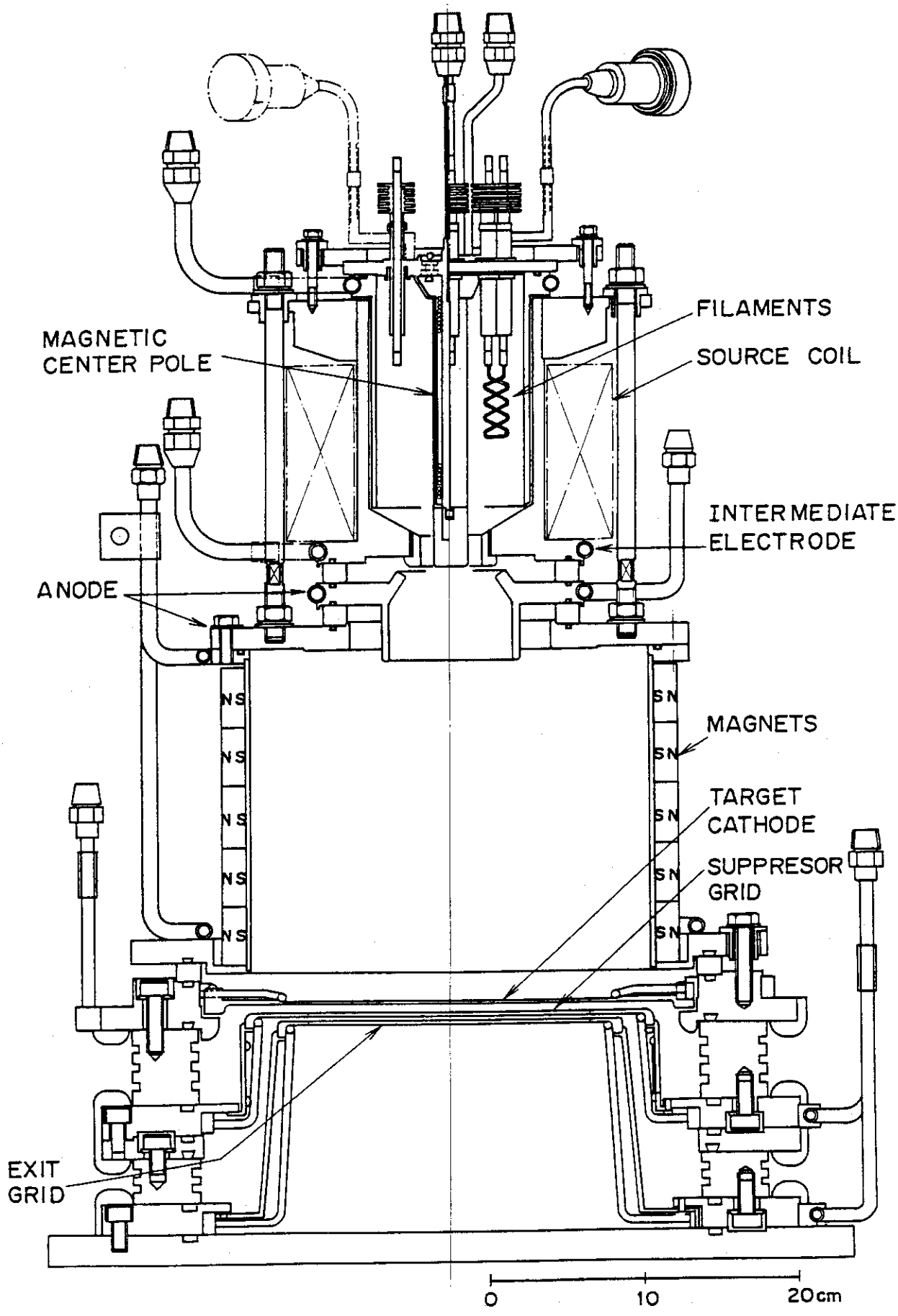

Fig. 4 Coaxial duoPIGatron ion source.

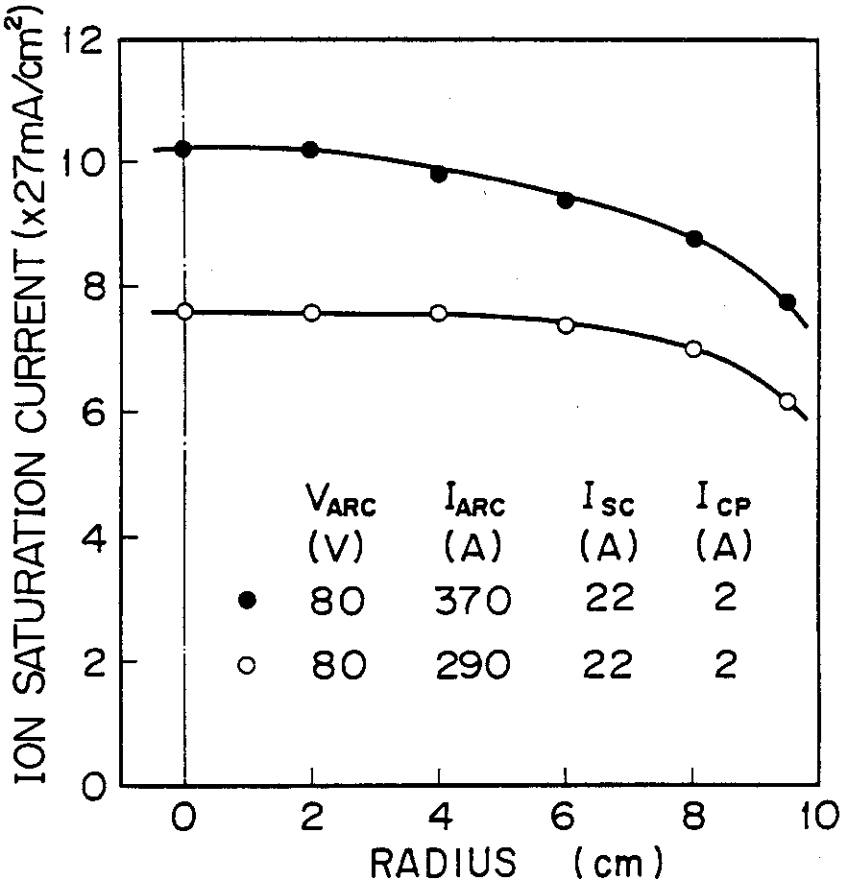

Fig. 5 Typical density profiles of the source plasma in the coaxial duoPIGatron source.

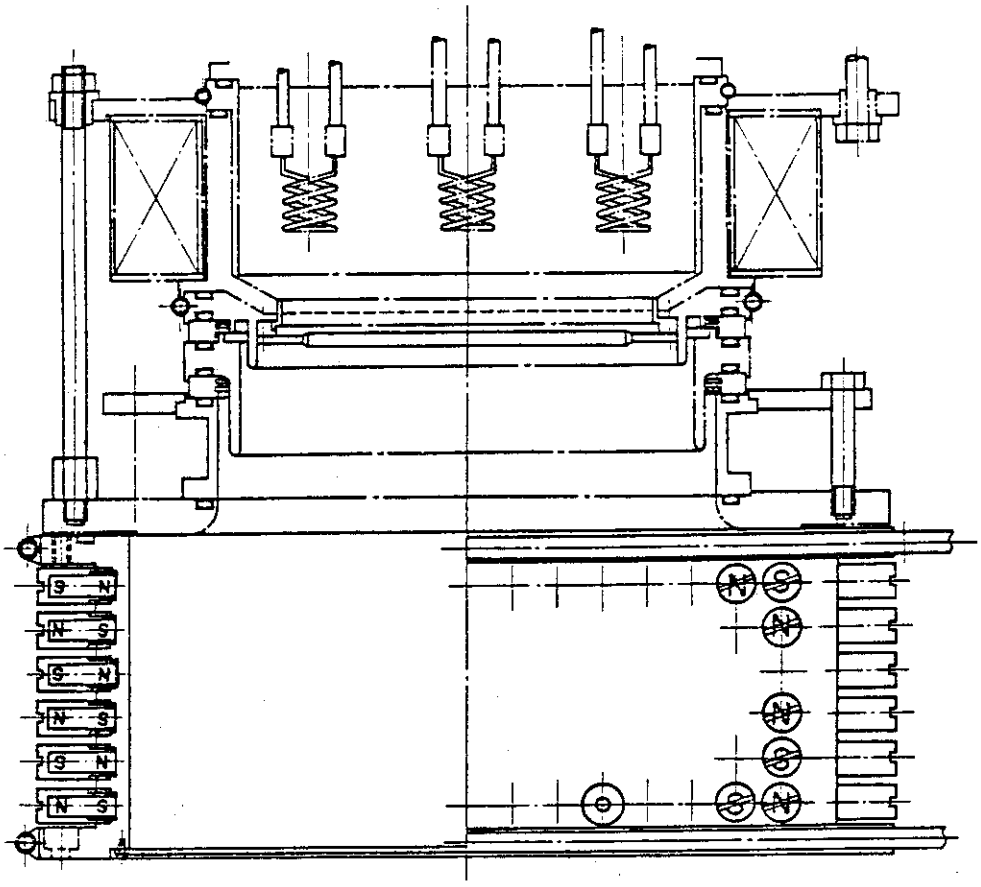

Fig. 6 Rectangularly-shaped duoPIGatron source.

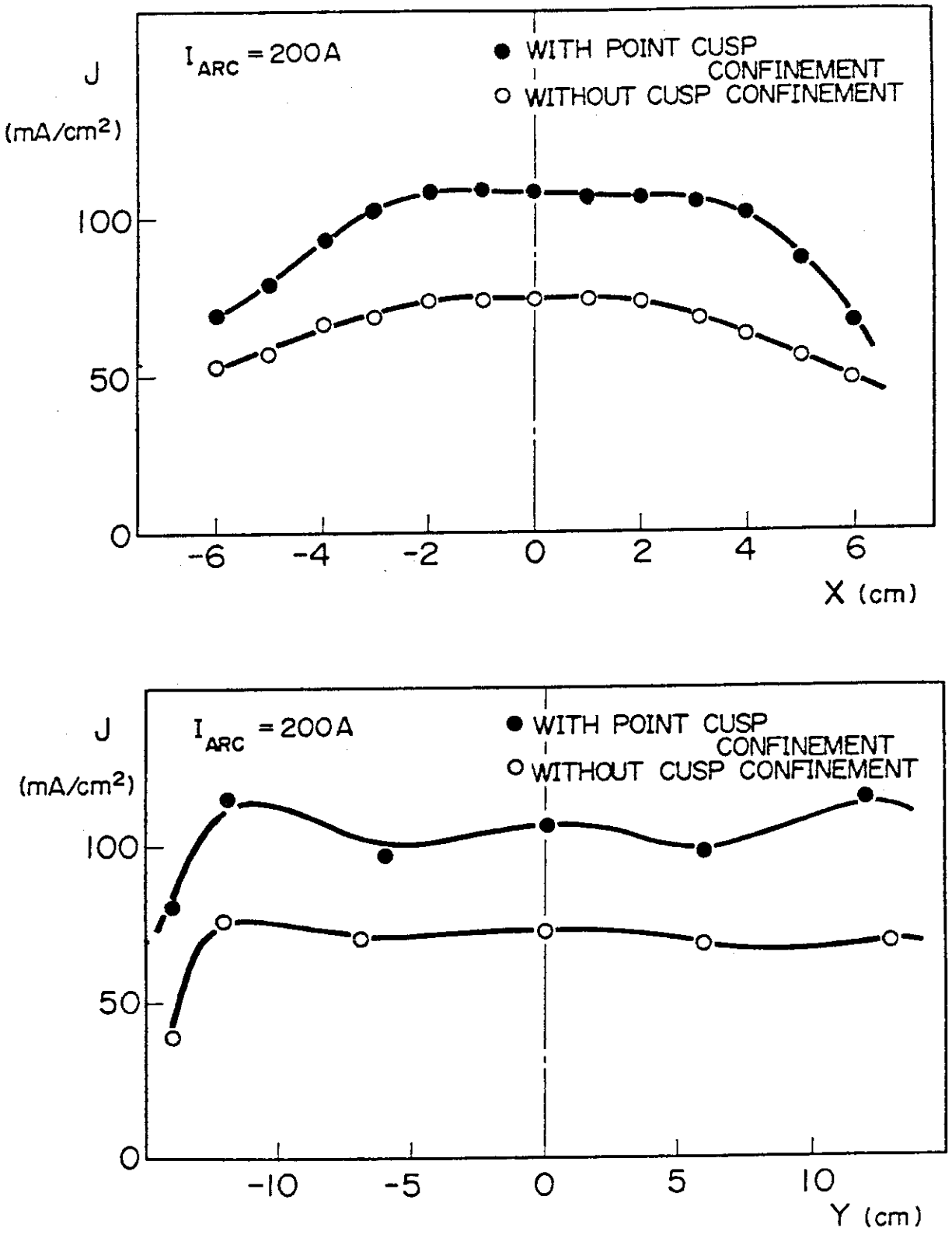

Fig. 7 A comparison of the density profiles with and without point cusp confinement.

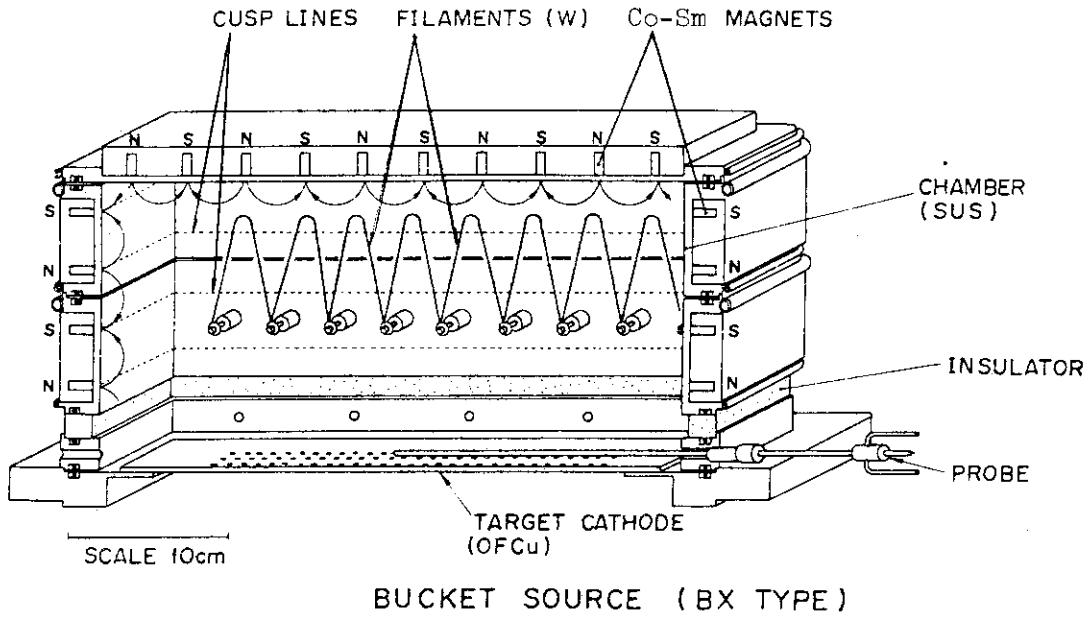

Fig. 8 Rectangularly-shaped bucket source at JAERI.

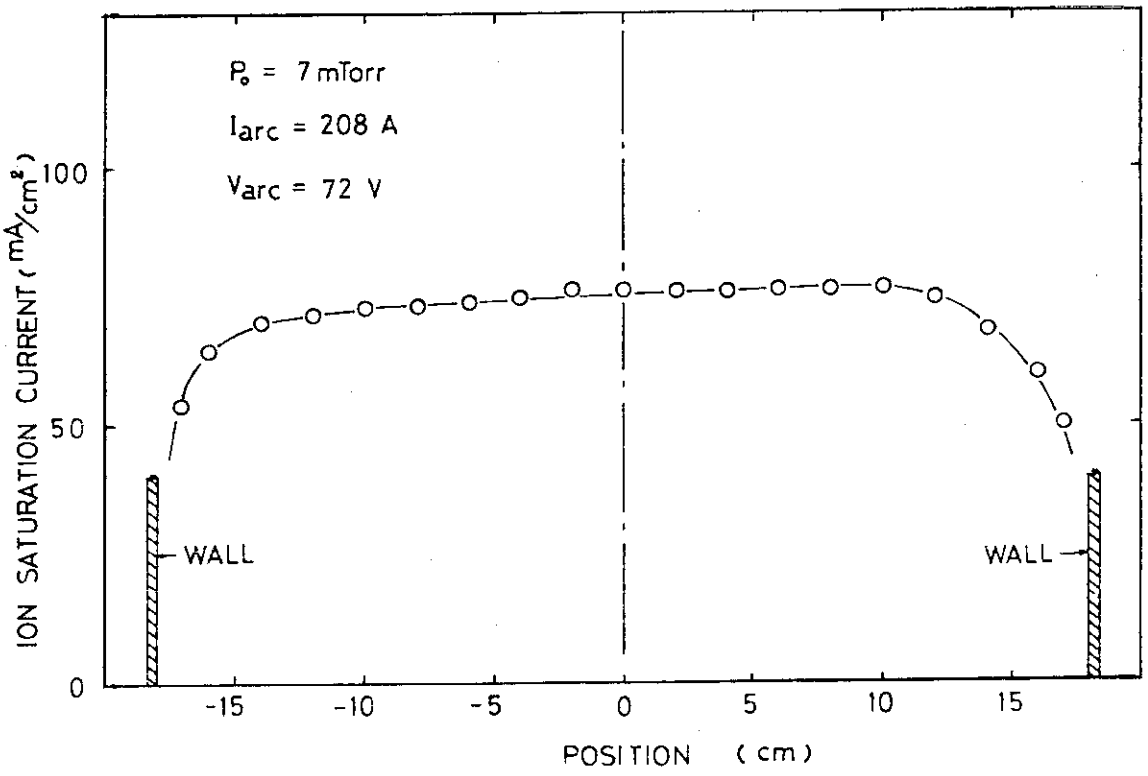

Fig. 9 A typical density profile of the source plasma in the rectangular bucket source.

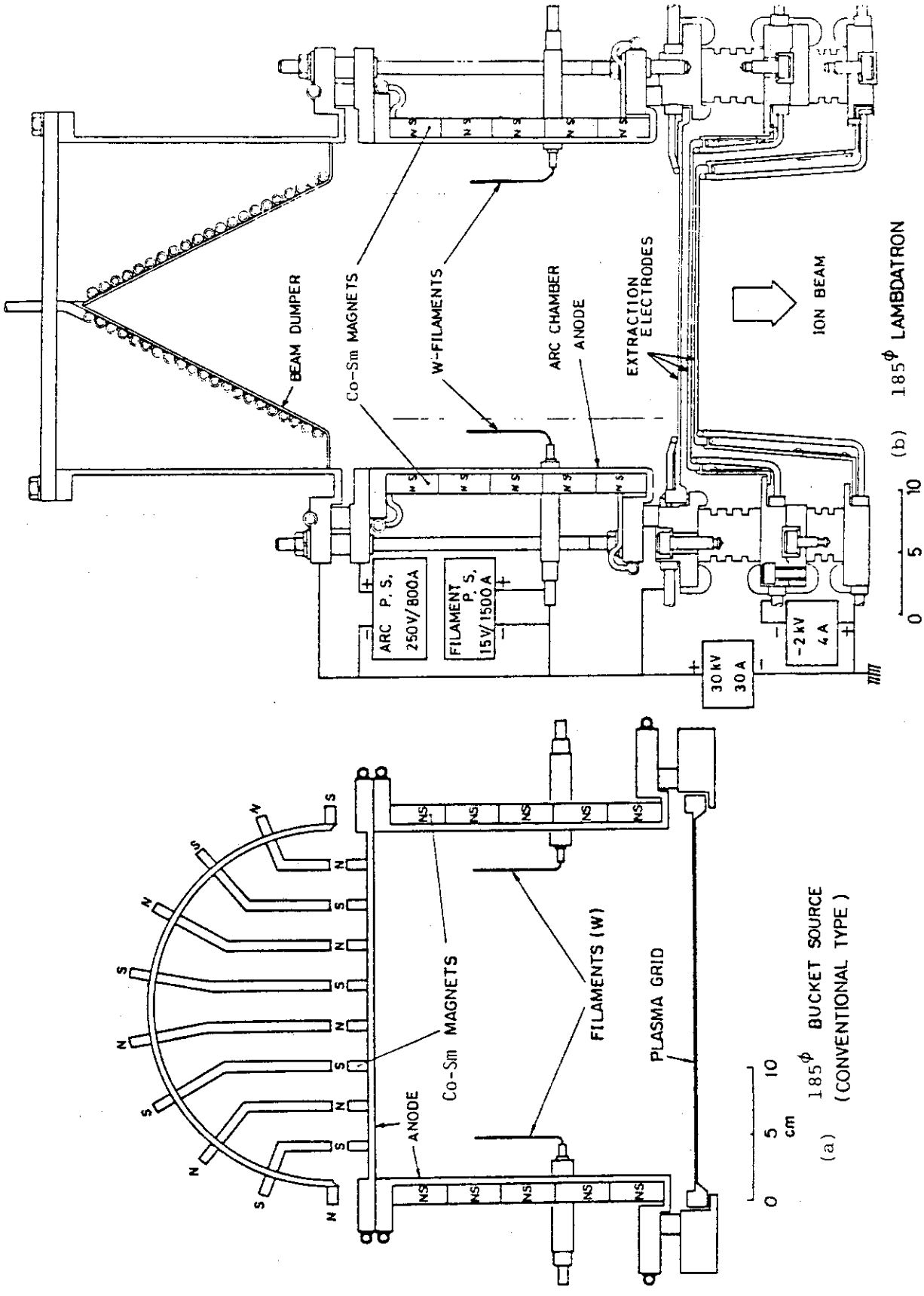

Fig. 10 Schematic of the circular bucket source (a) and the circular Lambdatron ion source (b).

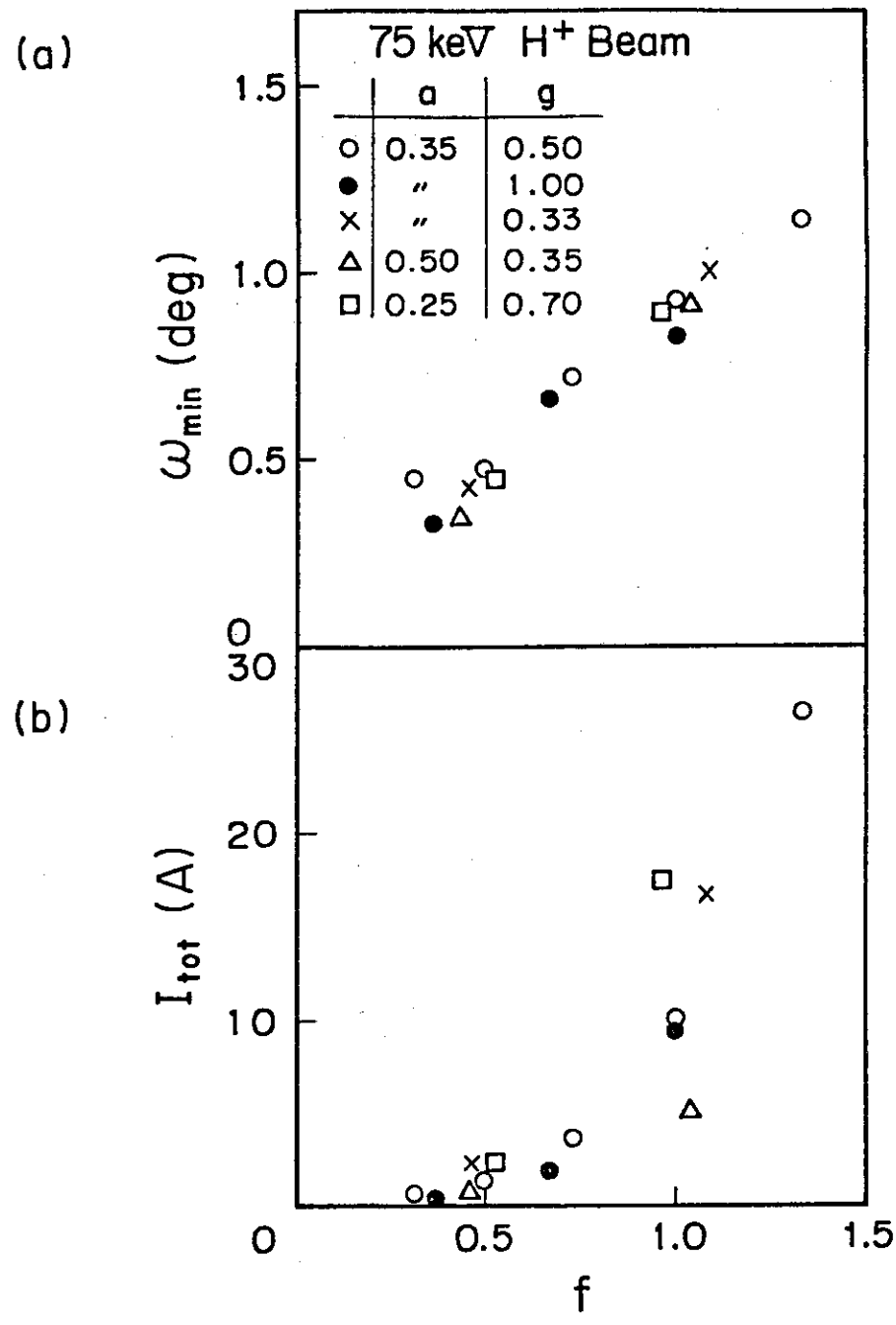

Fig. 11 Dependence of the minimum divergence on the field intensity ratio f (a), and the dependence of the total extracted current from the 12-cm-diam. grids with 40% transparency on f.

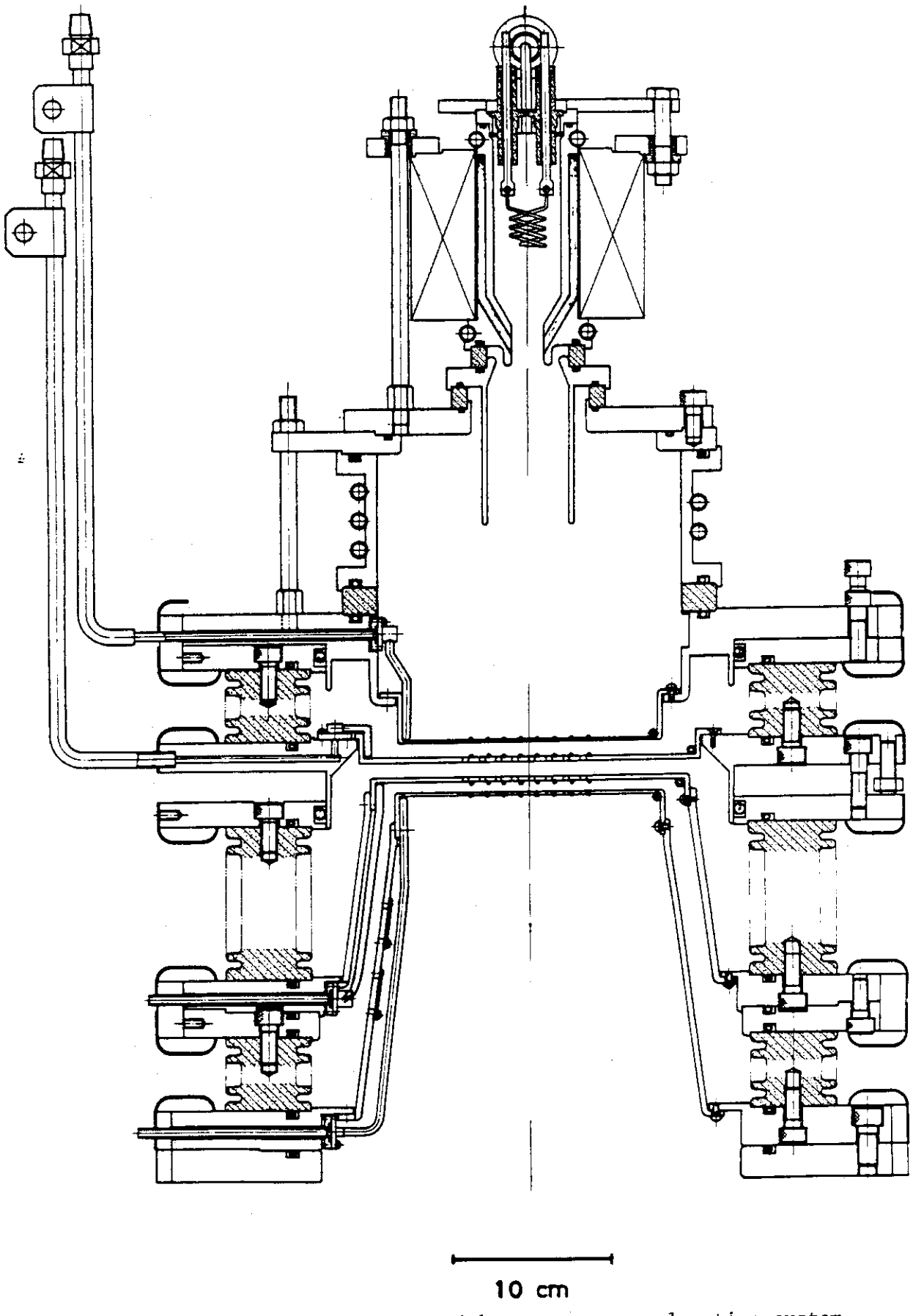

Fig. 12 DuoPIGatron ion source with two-stage acceleration system.

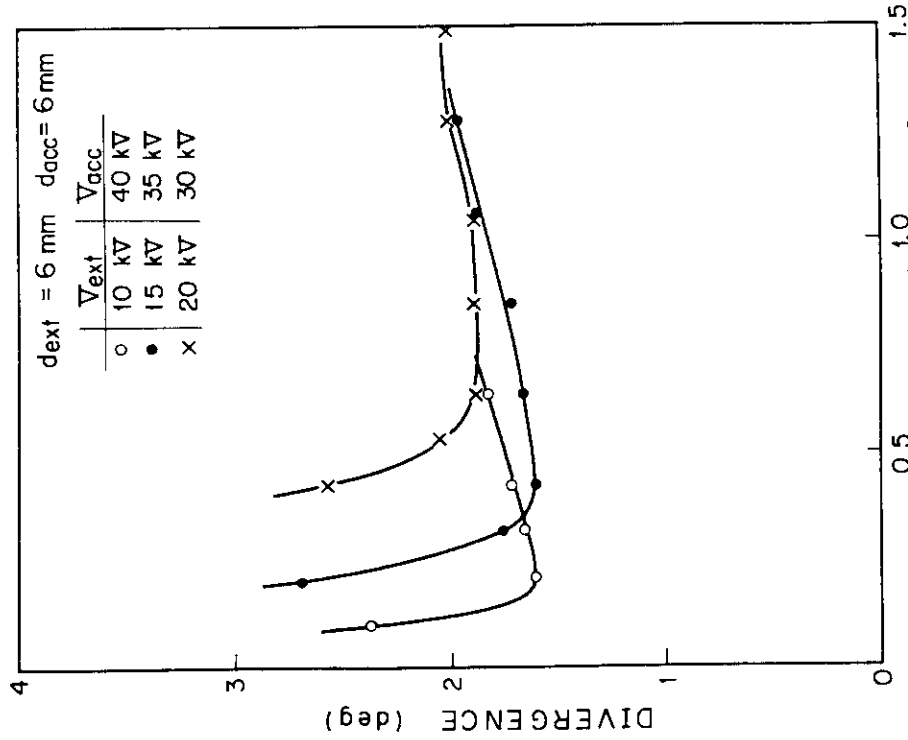

Fig. 14 Beam divergence as a function of perveance per hole, where total beam energy is fixed to 50 keV.

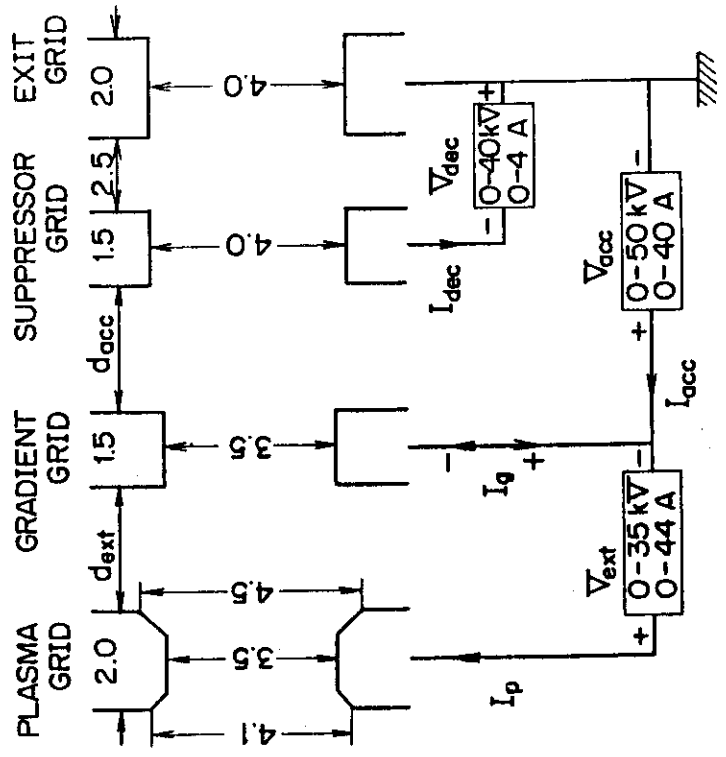

Fig. 13 Schematic of the two-stage acceleration system composed of four grids, and the power supply system.

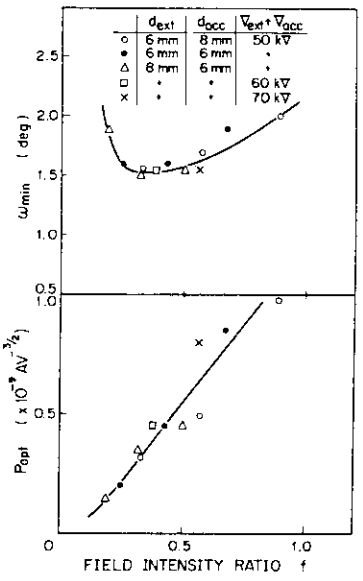

Fig. 15 Dependence of minimum beam divergence ω_{min} and optimum perveance Popt on the field intensity ratio.

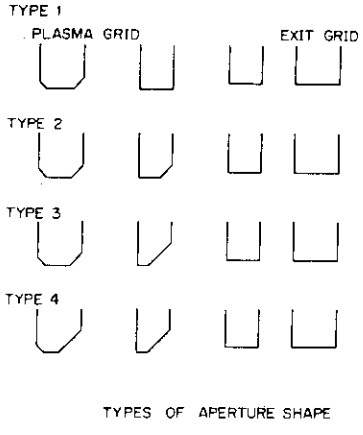

Fig. 16 Types of aperture shapes studied.

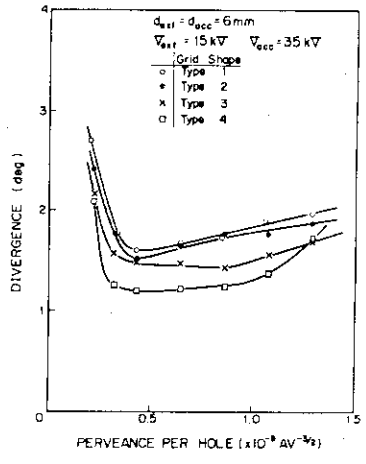

Fig. 17 Improvement of beam divergence by chamfering the aperture edges.

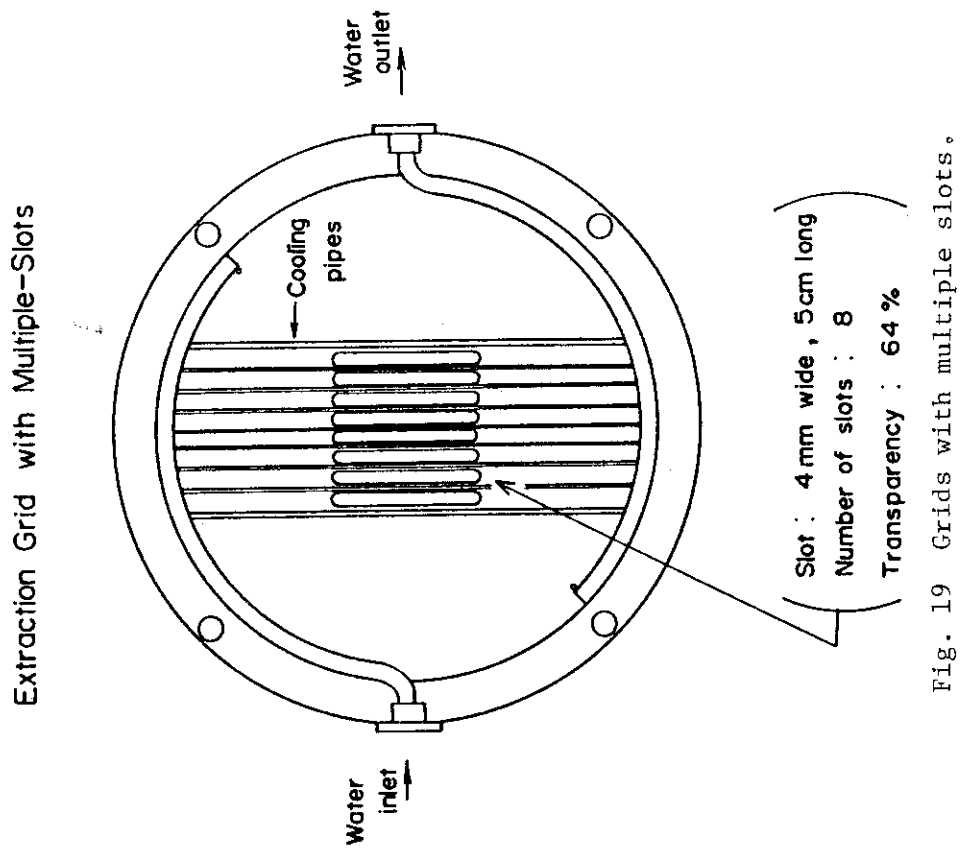

Fig. 19 Grids with multiple slots.

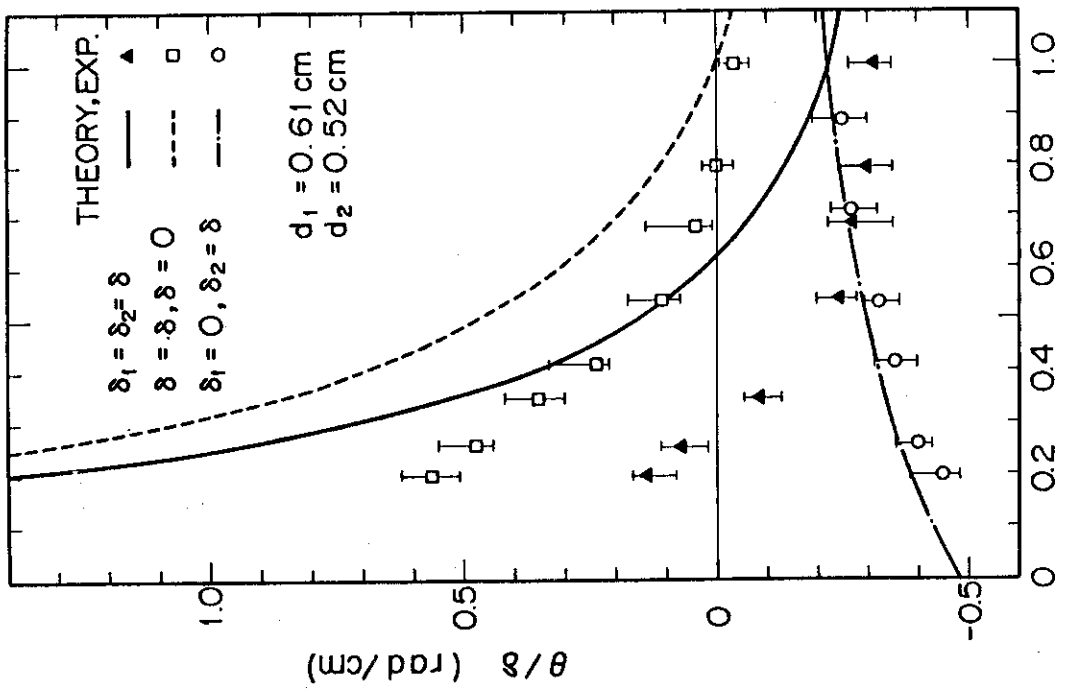

Fig. 18 Dependence of deflection characteristics on the field intensity ratio.

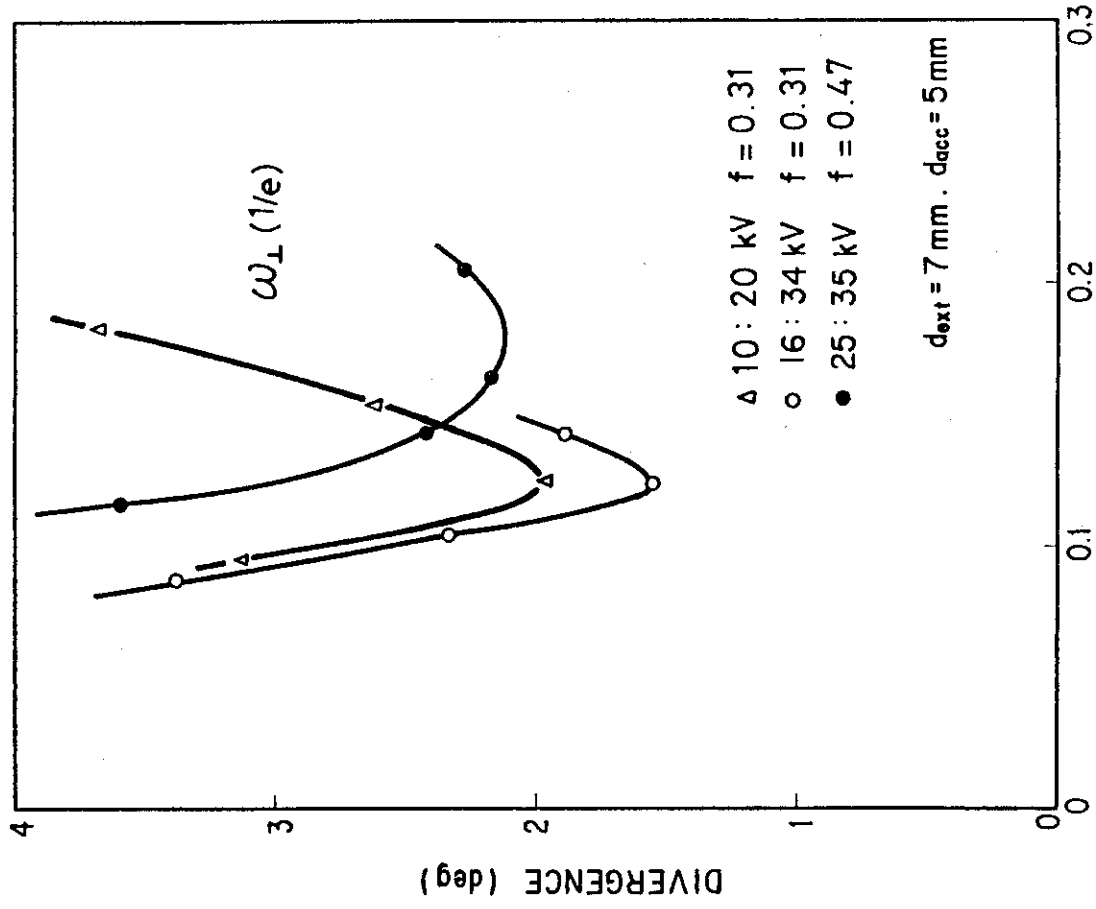

Fig. 21 Variations of the divergence in the direction perpendicular to the slots as a function of perveance.

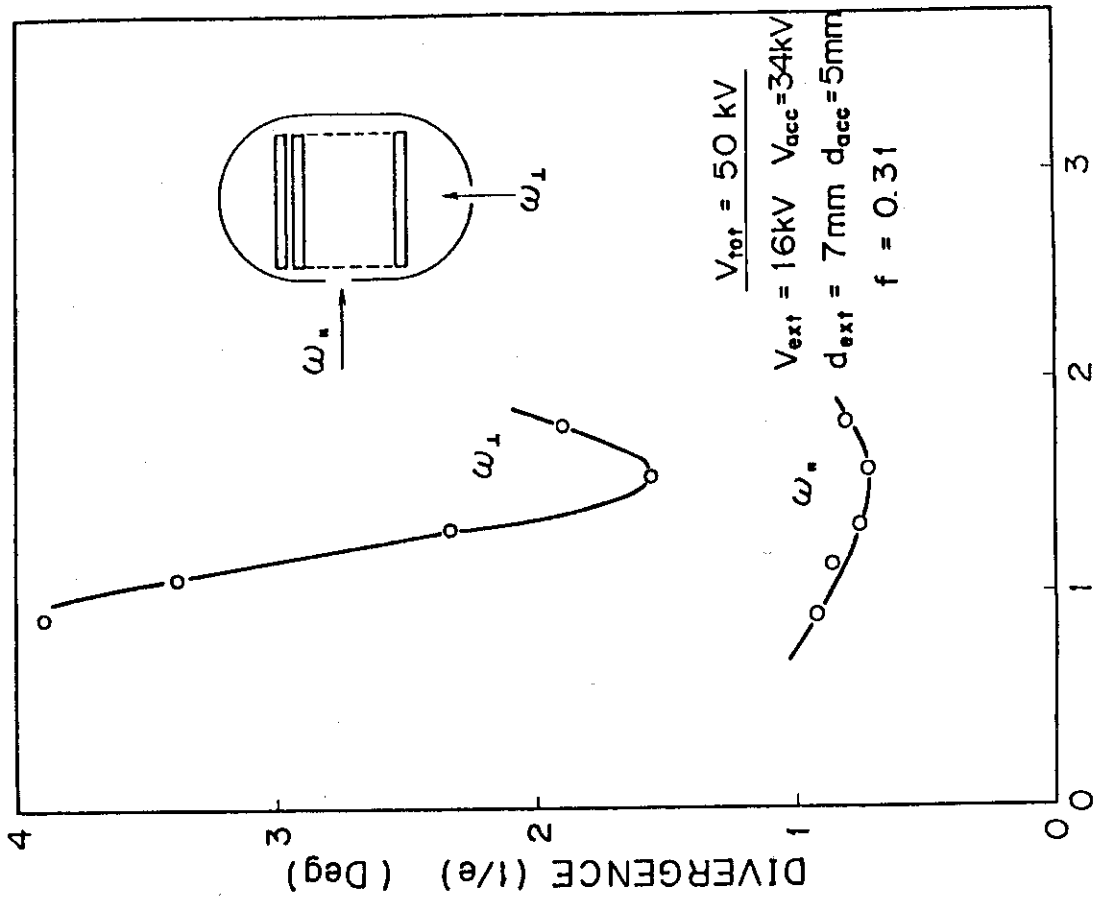

Fig. 20 Beam divergences in both directions perpendicular and parallel to the slots.

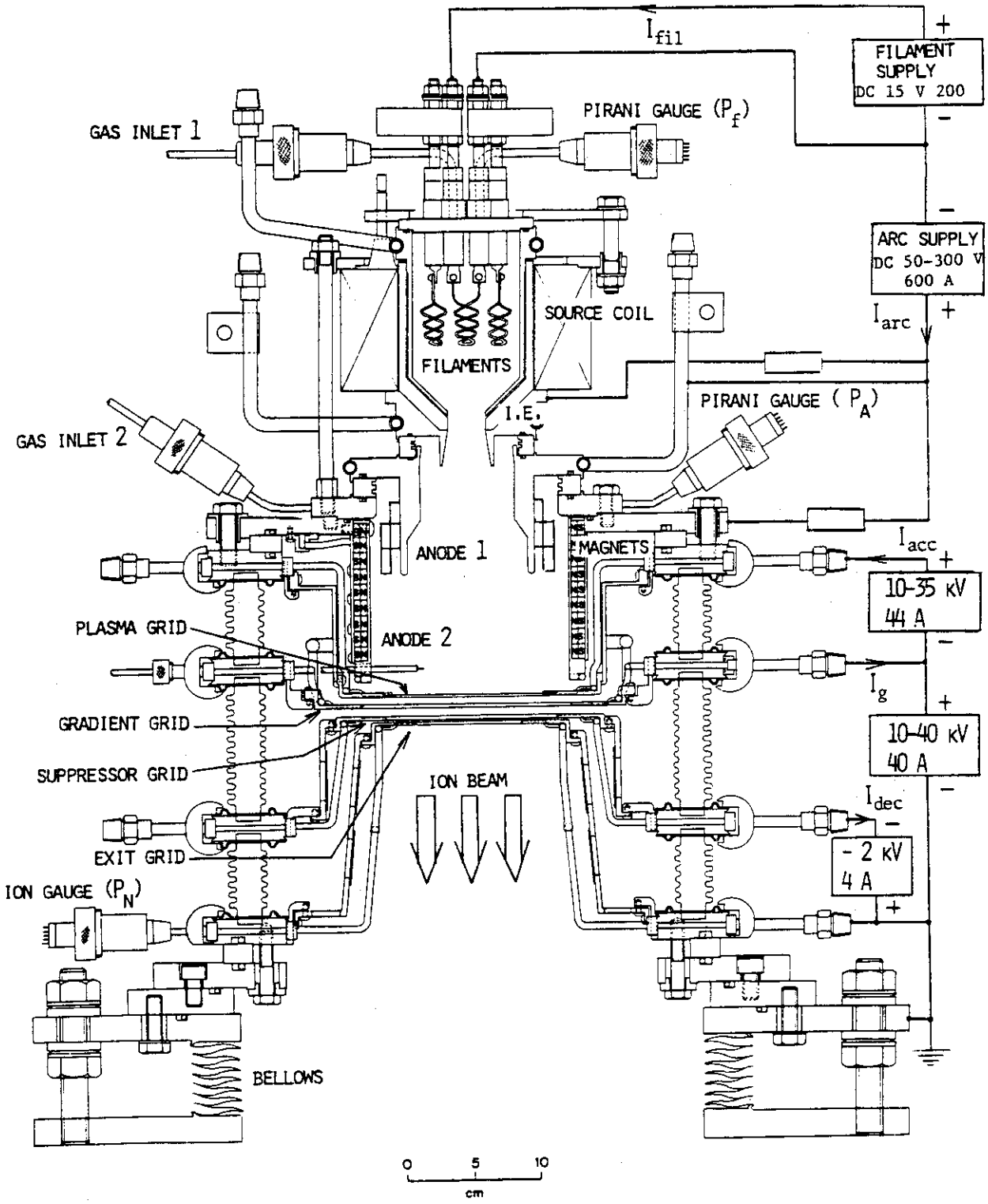

Fig. 22 Modified duoPIGatron ion source with two-stage accelerator.

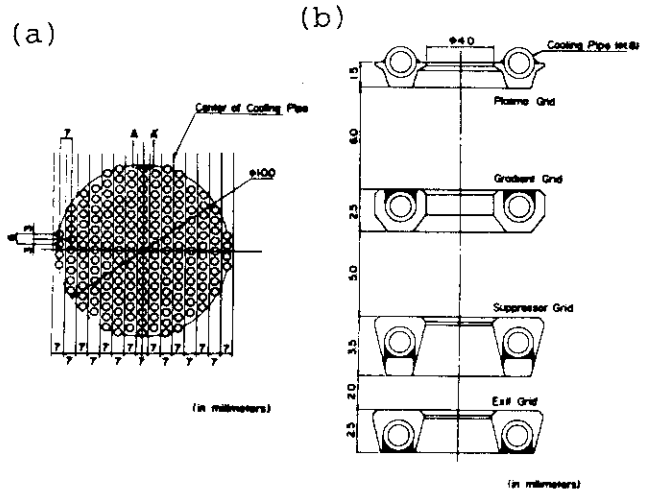

Fig. 23 Aperture pattern of a 10 cm diameter grid (a), and the crosssectional view of apertures in each grid (b).

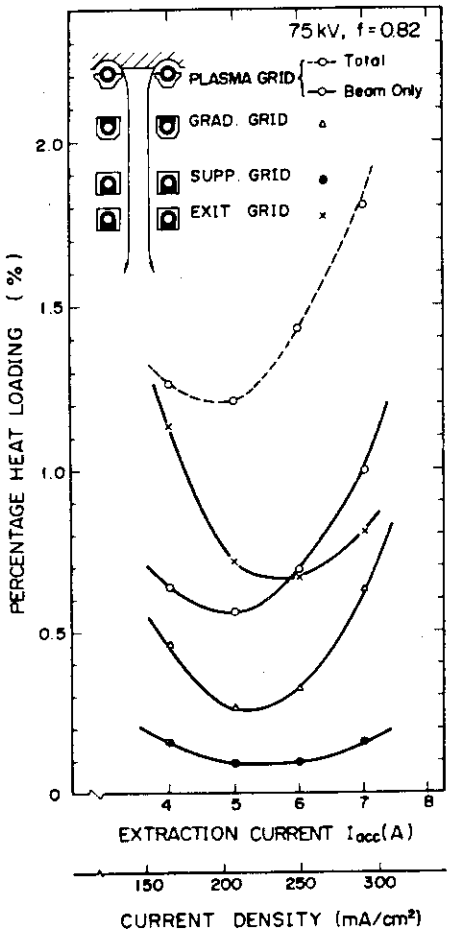

Fig. 24 Heat loading of each grid vs. extraction current at the beam energy of 75 keV.

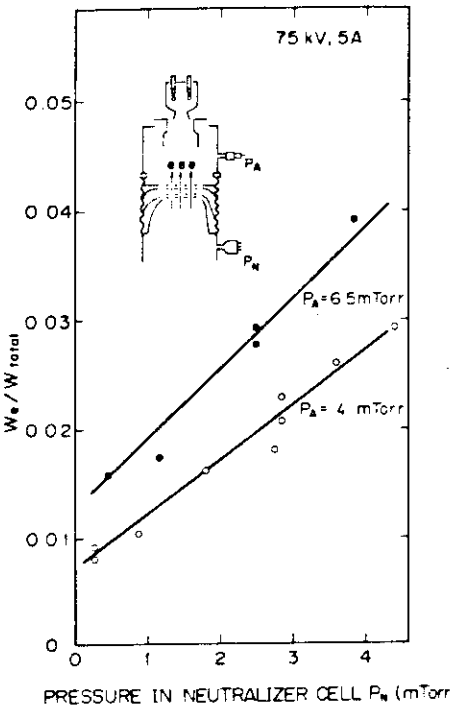

Fig. 25 Power flux of backstream electrons to the arc chamber vs. the gas pressure in neutralizer as a parameter of the pressure in the arc chamber.

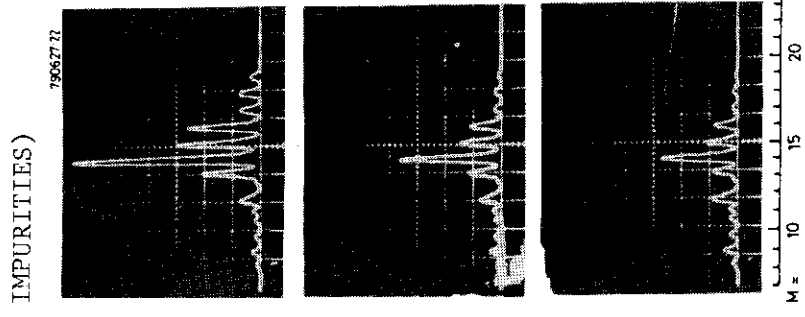

Fig. 26 Time dependence of mass spectra of the impurities related to carbon and oxygen.

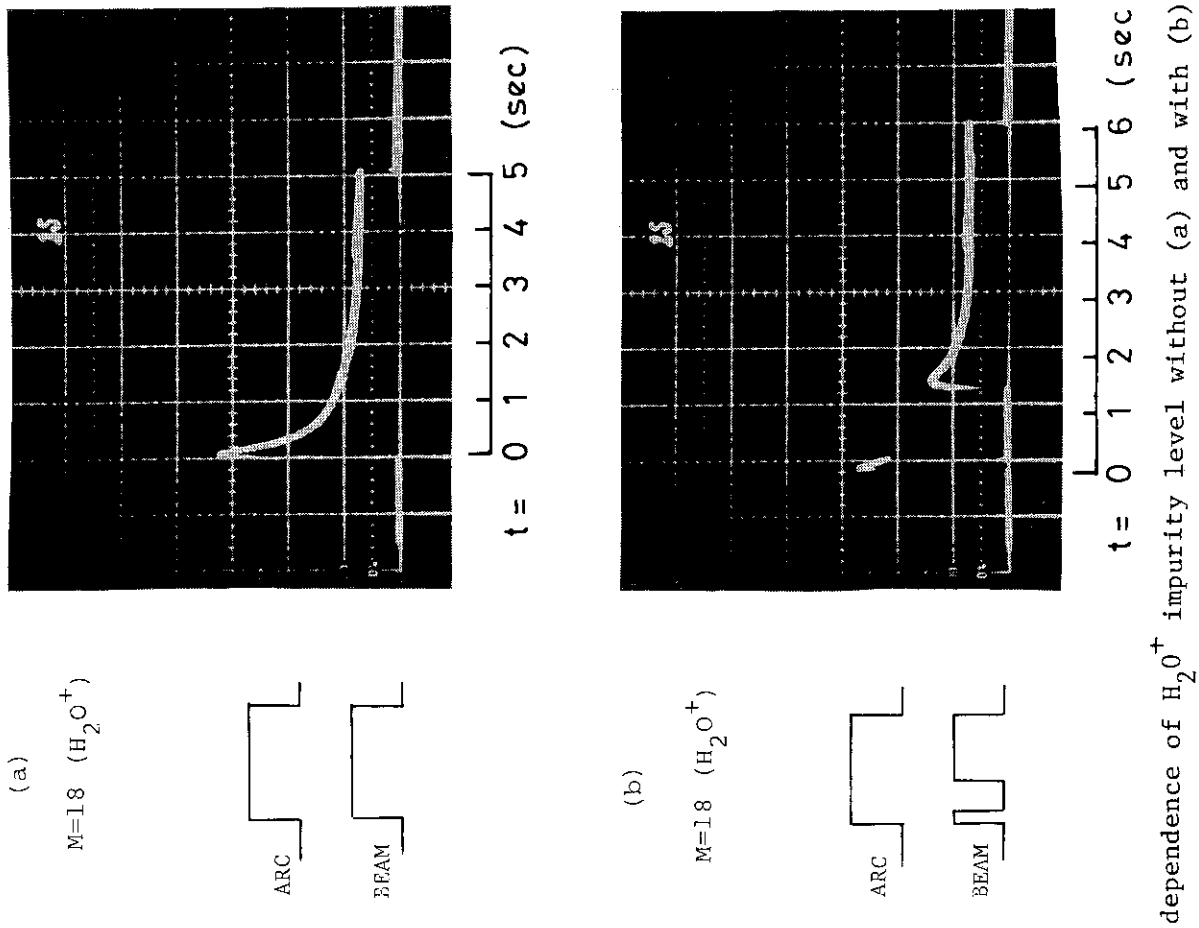

Fig. 27 Time dependence of H_2O^+ impurity level without (a) and with (b) arc flushing.

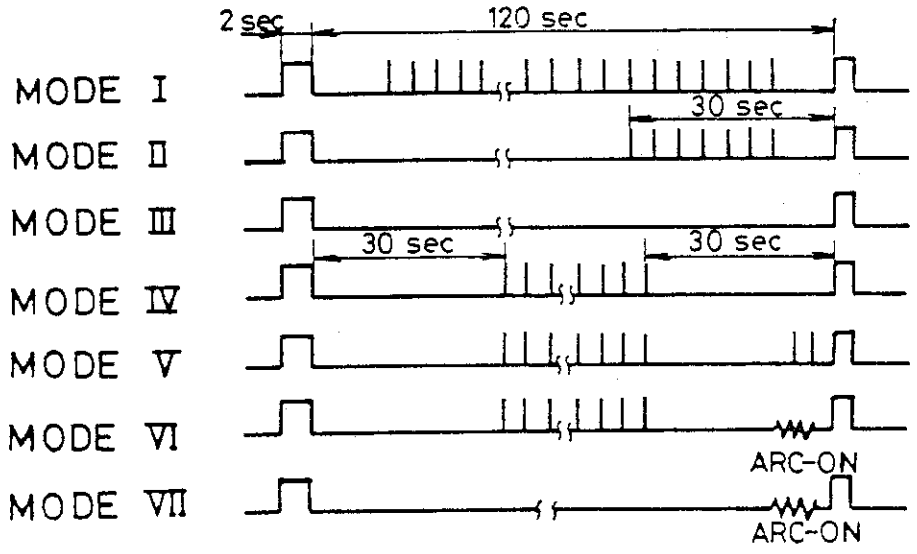

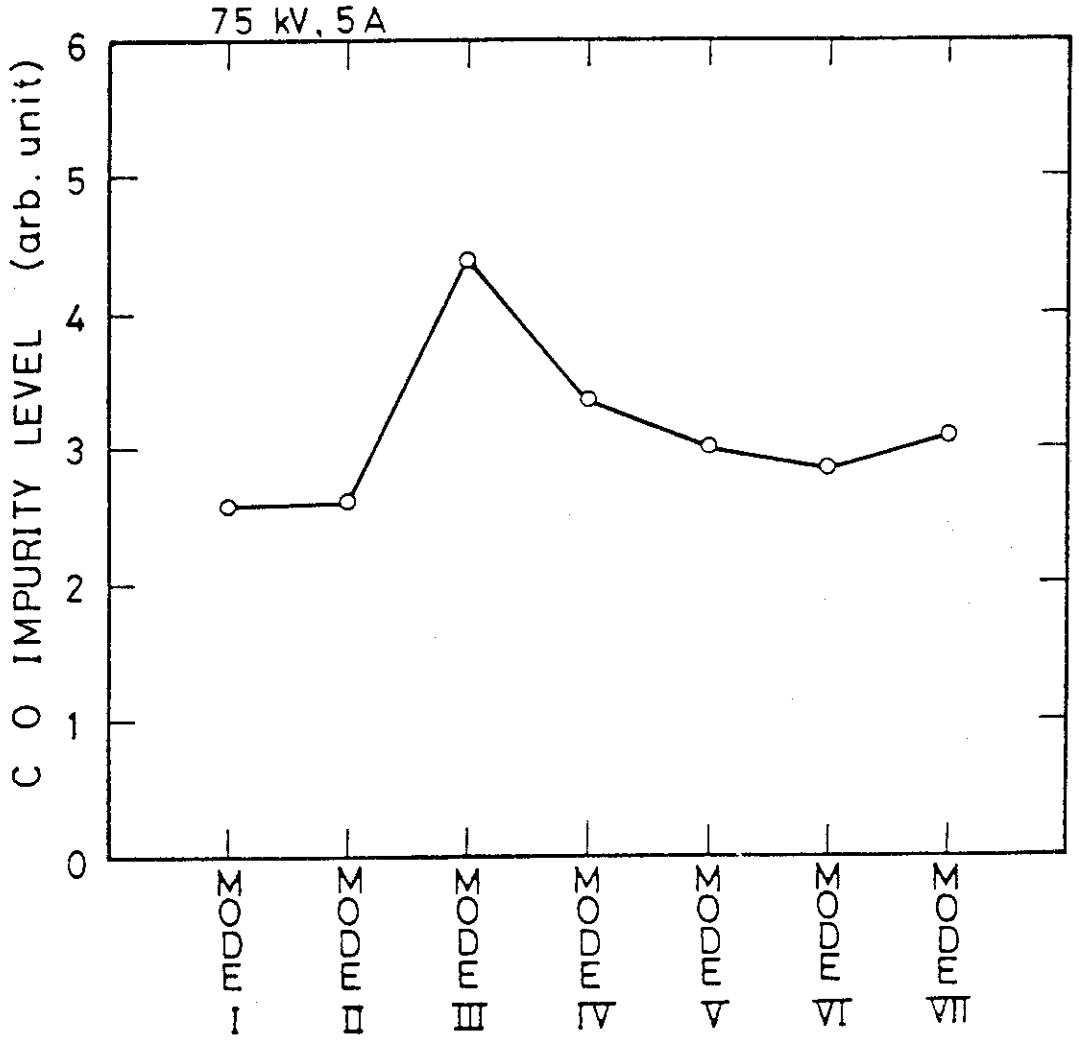

Fig. 28 Dependence of C, O impurity level on the various conditioning modes.

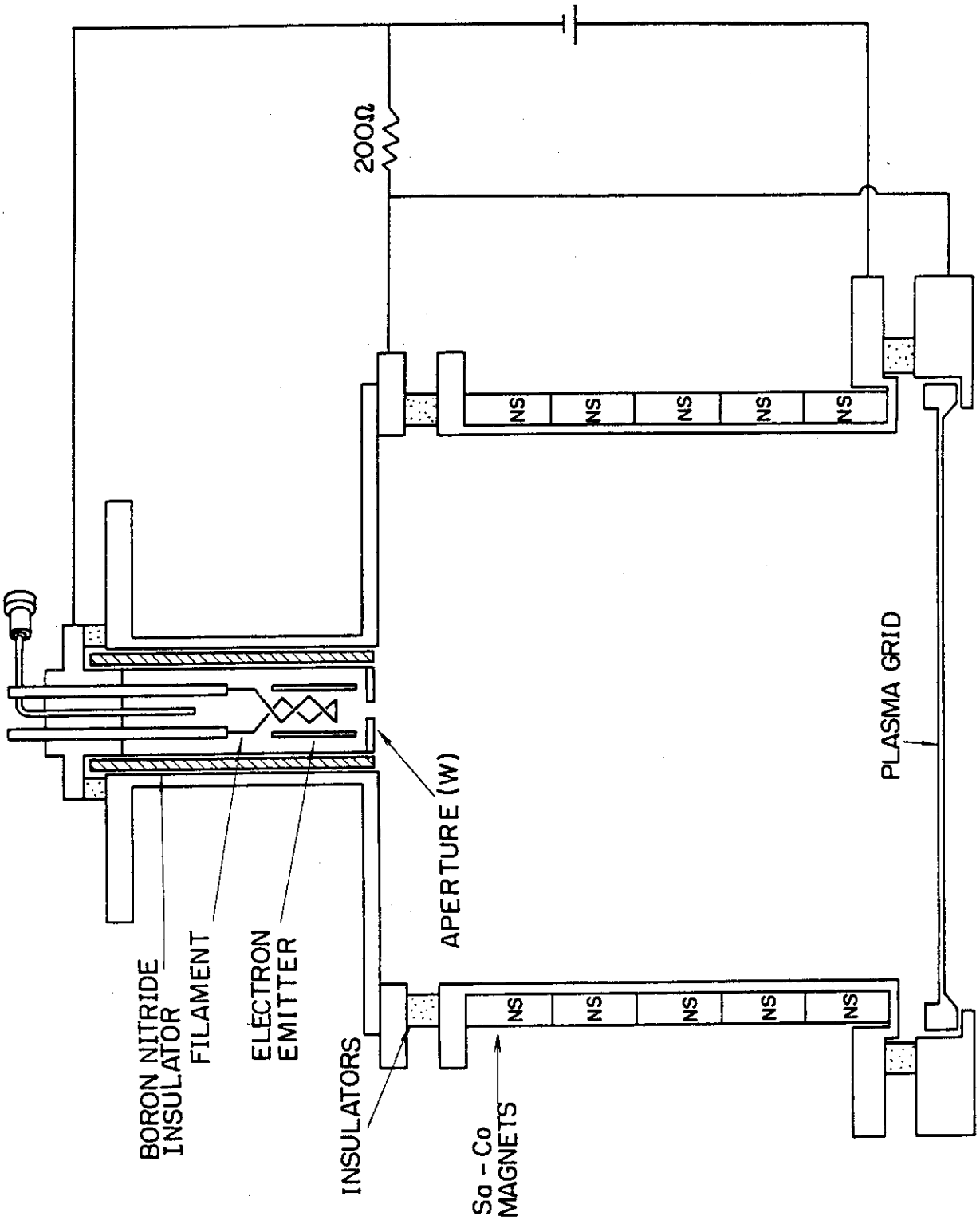

Fig. 29 Bucket source with a hollow cathode.

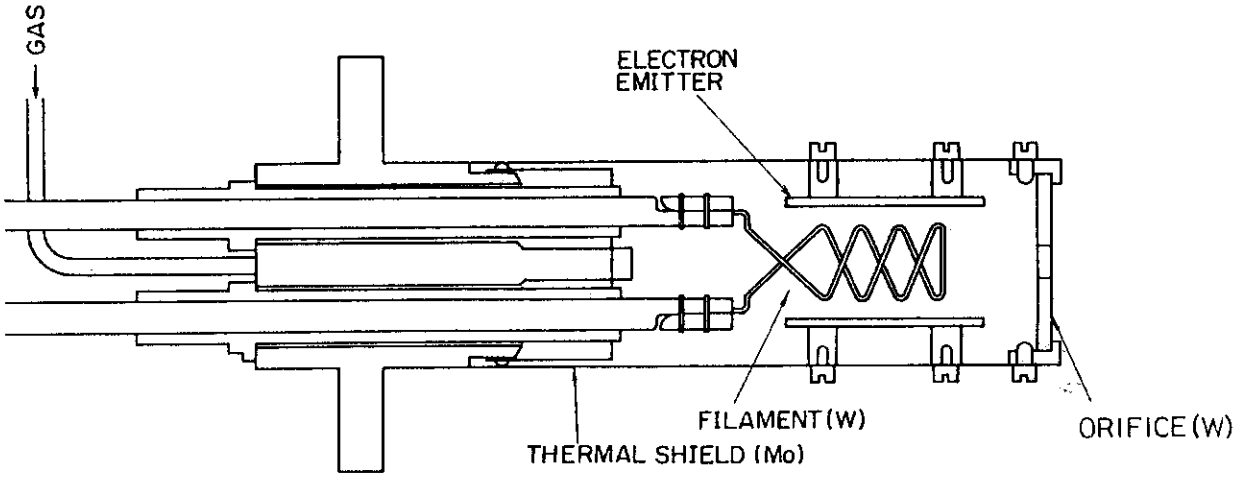

Fig. 30 Detail of the hollow cathode used and tested at JAERI.

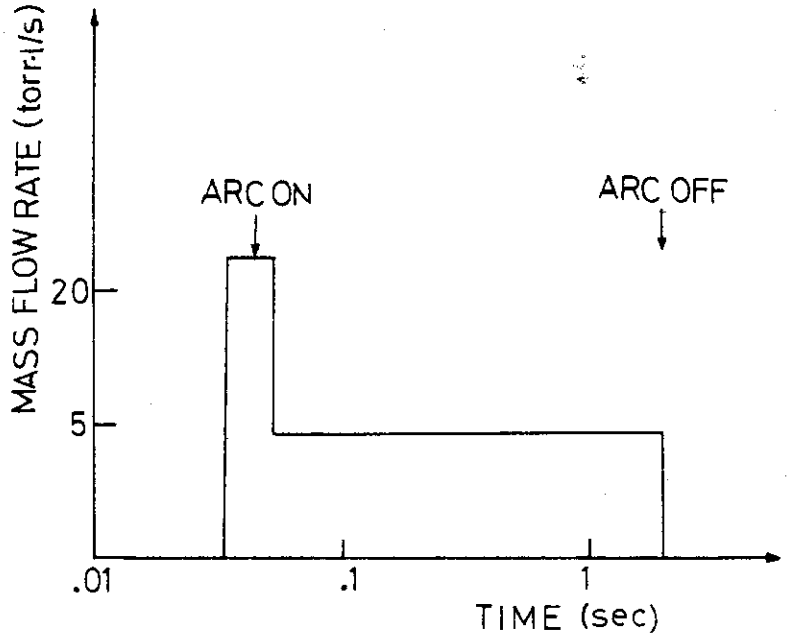

Fig. 31 Time dependence of gas flow through the hollow cathode.